Received: 30 October 2019 | Revised: 10 July 2020 | Accepted: 17 July 2020

DOI: 10.1002/eqe.3332

WILEY

RESEARCH ARTICLE

Seismic performance of dual systems coupling moment-resisting and buckling-restrained braced frames

Fabio Freddi[1] | **Enrico Tubaldi**[2] | **Alessandro Zona**[3] | **Andrea Dall'Asta**[3]

[1]Department of Civil, Environmental and Geomatic Engineering, University College London, London, UK

[2]Department of Civil and Environmental Engineering, University of Strathclyde, Glasgow, UK

[3]School of Architecture and Design, University of Camerino, Ascoli Piceno, Italy

Correspondence:
Fabio Freddi, Department of Civil, Environmental and Geomatic Engineering, University College London, London WC1E 6BT, UK.
Email: f.freddi@ucl.ac.uk

Funding information
UK-India Education and Research Initiative; (UKIERI) joint research program, Grant/Award Number: 2017-UGC-10070

Summary

Buckling-restrained braces (BRBs) have proven to be very effective in improving the seismic performance of existing and new structures. They provide strength, stiffness and add energy dissipation to the structure. However, being BRBs characterized by a low post-elastic stiffness, their use may lead to residual deformations hindering the building's reparability and to excessive cumulative ductility demand possibly compromising the residual capacity of BRBs. To overcome these drawbacks, BRB frames (BRBFs) can be coupled with moment-resisting frames (MRFs) to form dual systems. If properly designed, MRFs acting as back-up frames allow the control of the residual drifts and the optimization of the performance of the BRBs. The contribution of this study is to provide insights into the performance and residual capacity of BRBFs-MRFs dual systems and to shed light on the influence of the main BRB's design parameters. To this end, a nondimensional formulation of the equation of motion is introduced for a single degree of freedom system, and an extensive parametric study is performed for a set of natural ground motion records with different characteristics and scaled to various intensity levels. This allows the investigation of a wide range of configurations, considering different levels of the relative strength and ductility demand of BRBFs and MRFs, and obtains useful information for their design. Finally, two case study frames, modeled as two-dimensional nonlinear multi-degree of freedom systems, are analyzed, and the results were compared to those obtained from the nondimensional formulation to show the capabilities and the limitations of the adopted methodology and of the SDOF approximation.

KEYWORDS

buckling-restrained braces, cumulative ductility, dual systems, moment-resisting frames, nondimensional analysis, seismic performance

1 | INTRODUCTION

Buckling-restrained braced frames (BRBFs) are earthquake resisting systems employing elasto-plastic passive energy dissipation devices, i.e., buckling-restrained braces (BRBs),[1,2] to resist the horizontal seismic forces and to dissipate the seismic energy. In a BRB, a sleeve provides buckling resistance to an unbonded core that resists the axial stress, and, as buckling is prevented, the BRB's core can develop axial yielding in compression in addition to that in tension ensuring an almost symmetric hysteretic behavior.[3–6] This allows developing large and stable hysteretic cycles contributing to the dissipation of the seismic energy. For this reason, the use of these devices is very effective for both new constructions and the rehabilitation of existing buildings.[7,8]

The large and stable energy dissipation capacity of BRBs, proven by many experimental campaigns,[5,6] is accompanied by a low post-yielding stiffness, which may result in inter-story drift concentration[9] and large residual inter-story drifts. In addition, experimental tests demonstrated the susceptibility of BRBs to low-cycle fatigue fracture due to the limited cumulative ductility capacity.[10,11] Both these effects can influence the residual capacity of the structure. Inter-story drift concentration is generally related to the nonregular distributions of the brace over-strength over the building height that can lead to soft story formation. Large residual drifts can significantly compromise the building reparability, leading to high repair costs and disruption of the building use or occupation.[12] While investigating the seismic performance of BRBFs, Sabelli et al[13] reported residual drifts values on average in the range of 40% to 60% of the peak drift, for example, 1.6% to 2.4% for a 4% peak drift. These values should be compared with the residual drift limit of 0.5% that, for building frames, is conventionally associated to building reparability based on post-earthquake reconnaissance.[14] Hence, BRBFs designed according to modern seismic codes under the Design Basis Earthquake, i.e., probability of exceedance of 10% in 50 years,[15] may exhibit residual drift values higher than this limit. In addition, large residual drifts and accumulation of ductility demand in the BRBs due to the mainshock may also jeopardize the building performance under aftershocks.[11] These issues, which may impair the cost-effectiveness of BRBFs, could be avoided, or limited, by using moment-resisting connections within the BRBF,[16] and/or by using steel moment-resisting frames (MRFs) in parallel with the BRBFs to create a dual system configuration.[17–25] Modern seismic codes, such as the SEI/ASCE 7-10,[26] encompass dual systems combining a stiff primary seismic force-resisting system (e.g., BRBF) with an MRF, as schematically represented in Figure 1. According to this code, the MRF in dual systems should be capable of resisting at least 25% of the prescribed seismic force.

Kiggins and Uang[17] investigated the seismic response of a three- and a six-story BRBFs with and without a parallel MRFs designed to resist 25% of the design base shear. The results show that MRFs in parallel allow the reduction of the residual drifts by about 50%, while providing similar performances in terms of peak inter-story drift demand, i.e,. to the formation of dual systems with the MRFs often co, with a reduction of the order of 10%. Similar results have been obtained also by Ariyaratana and Fahnestock[18] while considering a seven-story frame, where, also in this case, the MRF is designed to resist 25% of the total base shear. Aukeman and Laursen[19] assessed the significance of the SEI/-ASCE 7-10[26] design requirement for MRFs in dual systems and showed that even with MRFs resisting only 15% of the total base shear it is possible to achieve a good seismic performance. Mehdipanah et al[20] illustrated the importance of designing the BRBF and MRF subsystems with a suitable relative stiffness ratio to optimize the seismic performance. Maley et al[23] proposed a displacement-based design method for steel dual systems with BRBs and MRFs and tested its validity by performing nonlinear time-history analysis on four case studies whereas Barbagallo et al[24] recently proposed a seismic design method for dual structures with BRBs and MRFs with semi-rigid connections. Moreover, other

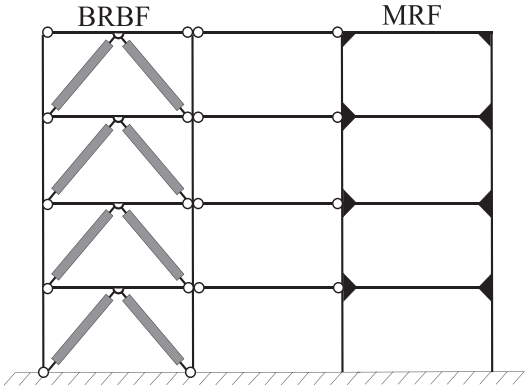

FIGURE 1 Dual system combining a buckling-restrained braced frame (BRBF) and a moment resisting frame (MRF)

authors[27,28] investigated the seismic performance and design methods for steel dual systems with conventional steel bracing and MRFs. In addition to the applications to newly designed steel frames, BRBs are also employed to enhance the lateral strength, stiffness, and the dissipation capacity of existing reinforced concrete (RC) buildings,[8,29,30] leading to the formation of dual systems with the MRFs often contributing more than 25% of the total base shear.

The works discussed above evaluated the benefits of using MRFs in parallel with BRBFs to form dual systems by considering only a few specific case studies, without the exploration of a wider range of possible design solutions. This does not allow the definition of general indications regarding the influence of the strength ratio, stiffness ratio, and target design ductility of BRBFs and MRFs as well as the optimal choice of their values. Only recently, Guerrero et al[31] performed a statistical analysis including dual systems modeled as single degree of freedom (SDOF) oscillators subjected to a large set of ground motions records. This study provides insights on the influence of several design parameters such as the post-yielding stiffness ratio, the displacement ductility, and the lateral strength ratio, on the seismic response of the structures. However, the focus is mostly on the influence of the design parameters on the residual displacements, and additional studies are required to provide support for design recommendations.

It is noteworthy that both the lack of knowledge in this field and the need for further studies were highlighted in a recent report[32] from the European Convention for Constructional Steelwork (ECCS) on the development of the Eurocode 8.[15] The present work aims to provide additional insights to support the definition of guidelines and recommendations on the optimum combination of strength, stiffness, and ductility of BRBFs and MRFs in dual systems. For this purpose, the problem is approached by considering a simplified SDOF representation of the problem, providing general information about the performance for a wide range of control parameters. This representation, demonstrated suitable for low-rise frames under some regularity conditions,[33,34] allows the development of a nondimensional formulation of the problem and the identification of the limited number of characteristics nondimensional parameters that control the seismic performance. Engineering demand parameters (EDPs) such as the peak normalized response, the normalized residual displacements, the cumulative ductility demand in the BRBFs, and the absolute accelerations are considered. By varying the nondimensional problem parameters, the performance of a wide range of configurations can be explored under a set of ground motion records representative of the uncertain seismic input, scaled to a common value of the seismic intensity measure.[35] It is noted that some response parameters, such as the residual displacements, may exhibit larger dispersion due to record-to-record variability effects compared to other, as already shown by Ruiz-Garcia and Miranda[36] for the residual deformations of bilinear hysteretic systems. Thus, the reported parametric study results include not only the mean values but also the dispersion of the EDPs of interest. In order to provide useful recommendations for the optimal design of dual systems, different design choices are investigated, corresponding to various combinations of the ductility demand of BRBFs and MRFs, within the respective capacity limit. Finally, the generality of the findings and the model limitations are investigated by considering two realistic MRFs-BRBFs dual systems, whose response is evaluated using state-of-the-art finite element (FE) tools.

The major novelty aspects of the study are: (1) the use of a nondimensional formulation, allowing the exploration of a wide range of configurations and design solutions, for example, existing RC frames retrofitted with BRBs, newly designed steel MRFs-BRBFs dual systems, gravity frames with BRBs as the only horizontal resisting elements (previous studies considered separately specific structural typologies and investigated only a limited range of possible of designs); (2) the use of an advanced numerical model for the BRBs, accounting for both hysteretic and isotropic hardening and allowing the investigation of the effect of the design choices on the cumulative ductility demand of the devices (previous studies used simple elastic-perfectly plastic models neglecting the effect of the hardening which could have led to an overestimation of the residual drifts); and (3) the analysis of the dispersion of the results of the parameters of interest (an aspect that was overlooked in previous studies that focused only on the mean values of the response parameters).

2 | PROBLEM FORMULATION

2.1 | SDOF model

The equation of motion governing the seismic response of the SDOF dual system of Figure 2A can be expressed as

$$m\ddot{u}(t) + c\dot{u}(t) + f_f(t)\ddot{u}f_b(t) = -m \cdot \ddot{u}_g(t), \tag{1}$$

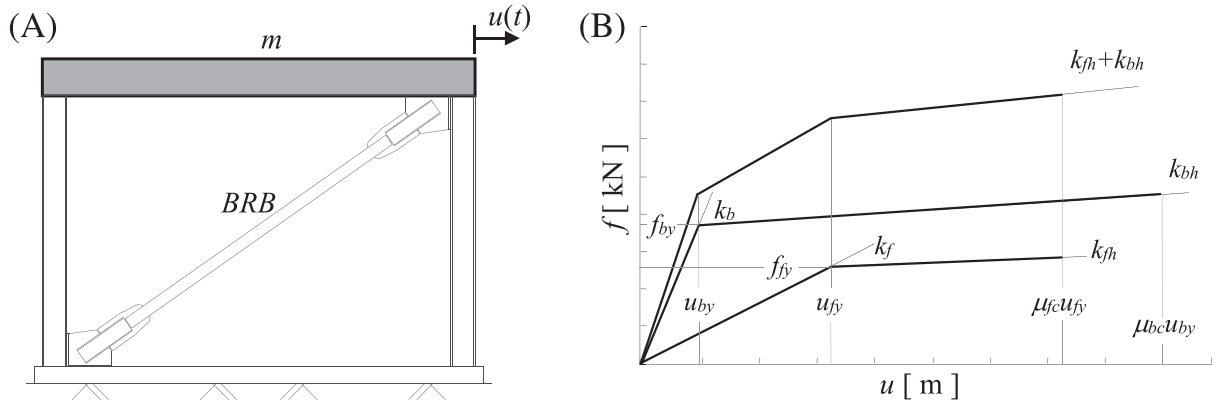

FIGURE 2 A, Single degree of freedom (SDOF) system of the dual moment-resisting and buckling-restrained braced frames and B, constitutive laws of the dual system

where m and c denote respectively the system mass and the inherent viscous damping constant of the system, $f_f(t)$ the resisting force of the MRF, $f_b(t)$ the resisting force of the BRBF, and $\ddot{u}_g(t)$ the ground acceleration input expected at the site.

The MRF is assumed to have an elasto-plastic behavior, with initial stiffness k_f, yielding force f_{fy}, yielding displacement $u_{fy} = f_{fy}/k_f$, ductility capacity μ_{fc}, and post-elastic stiffness k_{fh}. The BRBF is assumed to behave as a single BRB, and it is described by the BRB's elasto-plastic model developed by Zona and Dall'Asta.[3] This assumption is realistic only for BRBs yielding simultaneously at various stories, a condition which is usually sought in the design.[7,8,33] The Zona and Dall'Asta[3] model features both kinematic and isotropic hardening, the latter controlled by the cumulative plastic deformation. Moreover, it allows the description of the tension-compression asymmetry characteristic of the BRBs, where the maximum forces resisted in compression are typically about 10% to 15% higher than forces resisted in tension. However, it is worth mentioning that the asymmetry in the yielding strength and hardening behavior of the BRBs differs in general from manufacturer to manufacturer.[3] In this study, in order to keep the problem as simple as possible, the BRB's behavior is described only by the parameters which exhibit significant variation from device to device and that are explicitly reported in manufacturers catalogs, namely, initial stiffness k_b, initial yielding force f_{by}, initial yielding displacement $u_{by} = f_{by}/k_b$, and ductility capacity μ_{bc}. The values of the other parameters characterizing the kinematic and isotropic hardening as well as the different behavior in tension and in compression are assumed equal to those identified in Zona and Dall'Asta[3] based on the tests carried out by Tremblay et al.[5]

The MRF and BRBF modeled as SDOF systems are arranged in parallel (Figure 2B) to form a system which can describe a wide range of structural configurations and behaviors such as the case of BRBFs with moment-resisting connections,[16] BRBFs combined with MRFs to form a dual system,[17–25] or retrofit applications where BRBs are introduced within existing RC frames.[8,29]

The seismic input is characterized by significant uncertainties affecting not only its intensity but also the duration and frequency content. As usual, in Performance-Based Earthquake Engineering,[37] the seismic input is treated by introducing a random variable *IM* describing the intensity measure and a function $\ddot{u}_{g,1}(t)$ with $IM = 1$ describing the temporal evolution of the ground motion. Hence, the system response for a ground motion with an *IM* level *im* can be expressed as

$$m\ddot{u}(t) + c\dot{u}(t) + f_f(t) + f_b(t) = -m \cdot im \cdot \ddot{u}_{g,1}(t). \tag{2}$$

The choice of an appropriate *IM* for the problem should be driven by criteria of efficiency, sufficiency, and hazard computability.[35] In this paper, the spectral acceleration, $S_a(\omega_0, \xi)$, at the fundamental circular frequency of the system, ω_0, and for the damping factor ξ is employed as *IM*.

2.2 | Nondimensional form of the equation of motion

In order to reduce the number of variables to be considered in the parametric study, a nondimensional form of the equation of motion (Equation 2) is derived. For this purpose, the peak displacement of the system, u_{max}, under the fixed ground motion with history $\ddot{u}_{g,1}(t)$, can be expressed as

$$u_{max} = f\left(m, c, k_f, u_{fy}, k_b, u_{by}, im\right). \tag{3}$$

The eight variables of Equation 3 have dimensions $[u_{max}] = L$; $[m] = M$; $[c] = MT^{-1}$; $[k_f] = MT^{-2}$; $[u_{fy}] = L$; $[k_b] = MT^{-2}$; $[u_{by}] = L$; $[im] = LT^{-2}$ where the three physical dimensions are the time T, the mass M, and the length L. By applying the Buckingam Π-theorem,[38–43] Equation 3 can be conveniently reformulated in terms of dimensionless parameters, denoted as Π-terms. This approach permits the identification of the characteristic problem parameters that control the seismic response of the system also reducing the number of variables in Equation 3.

In the problem, there are three fundamental physical dimensions and eight dimensional variables. Thus, only 8–3 = 5 Π dimensionless parameters are needed. By selecting the systems mass m, the seismic intensity measure im, and the initial frame stiffness k_f as repeating variables, the following Π-terms are derived:

$$\Pi_u = \frac{u_{max} k_f}{m \cdot im}, \Pi_c = \frac{c}{\sqrt{m \cdot k_f}}, \Pi_{u_{fy}} = \frac{u_{fy} k_f}{m \cdot im}, \Pi_k = \frac{k_b}{k_f}, \Pi_{u_{by}} = \frac{u_{by} k_f}{m \cdot im}. \tag{4}$$

After manipulation of these terms, the following alternative set of Π-terms, which are given below a physical interpretation, can be obtained:

$$\delta = \frac{u_{max}\omega_0^2}{im}, \mu_f = \frac{u_{max}}{u_{fy}}, \mu_b = \frac{u_{max}}{u_{by}}, \xi = \frac{c}{2m\omega_0}, \alpha = \frac{f_{by}}{f_{fy}}, \tag{5}$$

where ${\omega_0}^2 = (k_b + k_f)/m$ denotes the square of the circular frequency of the SDOF dual system. It is noteworthy that in Equations 5, the first three parameters depend on the system response. The choice of the nondimensional parameters facilitates the performance assessment described in the next section.

The parameter δ denotes the peak displacement demand u_{max} normalized with respect to the displacement value $im/{\omega_0}^2$. By considering $S_a(\omega_0, \xi)$ as IM, δ can be interpreted as the displacement amplification factor, being the ratio between the maximum displacement of the linear system u_{max} and the pseudo-spectral displacement $S_d(\omega_0, \xi) = S_a(\omega_0, \xi)/{\omega_0}^2$, which is the maximum displacement of a linear system with the same initial stiffness and damping ratio ξ. The parameters μ_f and μ_b denote the ductility demand respectively of the MRF and the BRBF. The parameter α, representing the ratio between the yield strength capacity of the bracing system and that of the frame, was already employed in Freddi et al[8] while evaluating the seismic performance of a RC frame retrofitted with BRBs. The strength ratio considered in SEI/ASCE 7-10[26] to define a dual system is equal to

$$\frac{f_{fy}}{f_{by} + f_{fy}} = \frac{1}{\alpha + 1}. \tag{6}$$

Thus, based on the minimum base shear contribution of 25% required for the MRF by SEI/ASCE 7-10,[26] the system can be considered as dual if the parameter α is lower than 3.

It is noteworthy that the parameters δ, μ_f, and μ_b of Equations 5 depend on the response of the system, and their maximum values can be assumed as EDP, whereas parameters α and ξ are independent from the response. Other EDPs of interest for the performance assessment can be derived from the nondimensional solution. In particular, the following EDPs are considered:

$$\mu_{b,cum} = \frac{u_{bp,cum}}{u_{by}}, \delta_{res} = \frac{u_{res}}{u_{max}} \ , \ \alpha_{abs} = \frac{a_{max}}{im} \ , \tag{7}$$

where $\mu_{b,cum}$ denotes the cumulative ductility demand defined by the cumulative plastic displacement demand $u_{bp,cum}$ of the BRBF normalized with respect to its yielding displacement, δ_{res} the ratio between the residual and the peak displacement of the system u_{max}, and α_{abs} the absolute peak acceleration a_{max} normalized by the seismic intensity *im*.

3 | PERFORMANCE ASSESSMENT METHODOLOGY

The objective of the study is to evaluate how the circular frequency ω_0, the frame damping ratio ξ, the parameter α, and the values of the target ductility demand of the BRBF and of the MRF,[8,9] respectively, μ_{bt} and μ_{ft}, affect the performance of the system. In order to achieve this objective, it is not possible to follow the approach conventionally followed in other studies,[39–43] where a free variation of the nondimensional problem parameters is considered. This is because the two nondimensional parameters related to the response, μ_{bt} and μ_{ft}, are defined by the design condition and hence fixed a priori rather than being observed. This problem is an extension, to the system at hand, of the well-known and widely investigated problem of finding constant-ductility inelastic displacement ratios for elasto-plastic systems (see, e.g., Miranda[44]). It is an extension in the sense that the investigated system is more complex being a dual one, multiple response parameters are considered (not only the inelastic displacement ratio), and their statistical distribution is of interest (not only the mean value).

The procedure illustrated below solves the following problem: Given the system properties independent from the response ω_0, α, and ξ, find the values of the normalized peak displacement demand δ and of the other response parameters such that $\bar{\mu}_f = \mu_{ft}$ and $\bar{\mu}_b = \mu_{bt}$, where the overscore denotes the mean across the samples for the different records of the ground motion set. The procedure consists in the following steps:

1. Assign arbitrary target mean values to the peak mean displacement demand $\bar{u}_{max,t}$ and to the mass m, e.g., $\bar{u}_{max,t} = 1$ m and $m = 1$ ton. The obtained results are independent from the choice of these values. The corresponding values of the parameters of the physical system are

$$c = 2m\omega_0\xi,\ u_{fy} = \bar{u}_{max,t}/\bar{\mu}_f,\ u_{by} = \bar{u}_{max,t}/\bar{\mu}_b,\ k_f = \omega_0^2 m/\left(1 + \alpha u_{fy}/u_{by}\right),\ k_b = (\alpha u_{fy}/u_{by})k_f,$$

2. Scale the records to a common value of the intensity measure, e.g., $im = 1$;
3. Perform nonlinear dynamic analyses for the different records of the ground motion set;
4. Evaluate the mean value of the peak displacement response $\bar{u}_{max}$. If $\bar{u}_{max}$ is equal to the target value $\bar{u}_{max,t}$, then go to step 5. Otherwise, multiply *im* by the ratio $\bar{u}_{max,t}/\bar{u}_{max}$ and restart from step 2. This procedure corresponds to a linear interpolation between the relation $\bar{u}_{max}$ and *im*. If this procedure does not converge, resort can be made to any optimization algorithm;
5. Evaluate the statistics of δ, δ_{res}, α_{abs}, and $\mu_{b,cum}$ for the identified *IM* level.

Steps 1 to 4 ensure that the design condition of the MRF and the BRBF attaining simultaneously their target performance under the design earthquake input is achieved. Step 5 corresponds to the evaluation of the statistics of the other response parameters of interest at this condition.

4 | PARAMETRIC STUDY

This section illustrates the results of the parametric study carried out to evaluate the performance of the dual system with MRF and BRBF. The performance of the systems corresponding to different values of ω_0, α, μ_{ft}, μ_{bt}, and ξ is assessed by also considering the constraint posed by the attainment of the design condition. The parameter ω_0 is varied in a range corresponding to values of the vibration period $T_0 = 2\pi/\omega_0$ between 0.1 and 4 s, although due to space

constraints, only the results corresponding to 0.3, 1, and 2 s are reported in the paper. The strength ratio α assumes values in the range 0–100. The lower bound $\alpha = 0$ represents the case of the bare frame, whereas the upper bound of $\alpha = 100$ represents the case where the contribution of the MRF is negligible, and it is possible to consider the system as a frame with "pinned" connections where the horizontal stiffness and resistance is provided only by the BRBF. The parameter μ_{ft} is varied in the range 1–4. The case $\mu_{ft} = 1$ corresponds to a design condition where the frame behaves in its elastic range under the design earthquake whereas the case $\mu_{ft} = 4$ corresponds to a high ductility demand for the frame under the design earthquake. The parameter μ_{bt} is assumed to vary in the range 5–20. Values of 15–20 are typical for the ductility capacity of a BRB device.[45] The lower bound of 5 is considered because often, such as in case of the seismic retrofit of RC frames,[8] the BRB devices are arranged in series with an elastic brace and this leads to reduced values of the ductility capacity, which can be as low as 5 for flexible braces.[7,46] Finally, in order to limit the parameters to be varied in the parametric analysis, the values for the damping factor and the post-elastic stiffness ratio of the frame are assumed constant and respectively as $\xi = 5\%$ and $k_{fh} = 5\%$.

The nonlinear behavior of the system at the design condition is affected mainly by the design parameters α, μ_{ft}, and μ_{bt}. For the benefit of the subsequent discussion and interpretation of the results, it is useful to introduce the concept of equivalent ductility demand μ_{eq} of the dual system. For the sake of simplicity, μ_{eq} is derived by neglecting the hardening behavior of the two systems. Under this assumption, the two components of the dual system behave as equivalent elastic-perfectly plastic systems leading to a total strength capacity equal to $f_{by} + f_{fy}$. The equivalent ductility can be derived by the equivalence between the areas under the response curve of the dual system and of the equivalent elastic-perfectly plastic system as

$$\mu_{eq} = \frac{\alpha + 1}{\frac{\alpha}{\mu_{bt}} + \frac{1}{\mu_{ft}}}. \tag{8}$$

The expression of Equation 8 shows that for a given value of the frame ductility demand μ_{ft}, the equivalent ductility demand μ_{eq} of the dual system increases by increasing α and μ_{bt} as shown in Figure 3. Obviously, for $\alpha = 0$, the equivalent ductility of the system coincides with that of the MRF, whereas for very high values of α, the target ductility of the BRBF is attained. It is also worth observing that for $\alpha = 3$, that is, the maximum BRBF to MRF strength ratio, according to SEI/ASCE 7-10,[26] and $\mu_{bt} = 20$, i.e., the maximum ductility capacity of the BRBF, μ_{eq} spans the interval from 3.5 to 10 by varying μ_{ft} in the range from 1 to 4. In reality, both the MRF and the BRBF usually exhibit a hardening behavior after yielding, and thus, Equation 8 provides only an approximate estimate of the equivalent ductility of the system.

4.1 | Seismic input description and analysis model

A set of 240 ground motions is used to achieve confident estimates of the median response and dispersion accounting for the record-to-record variability.[47] This set was selected by Baker et al[48] for the analysis of a variety of structural systems located in active seismic regions. The records are representative of a wide range of variation in terms of source to site distance (R) (from 8.71 to 126.9 km), soil characteristics (V_{s30} spans from 203 to 2016.1 m/s), and moment magnitude (M_w) (from 5.3 to 7.9). A large number of zeros acceleration points (i.e., 40 s) have been added at the end of each record in order allow the free vibrations to stop and to correctly capture the residual displacements. Pulse-like records

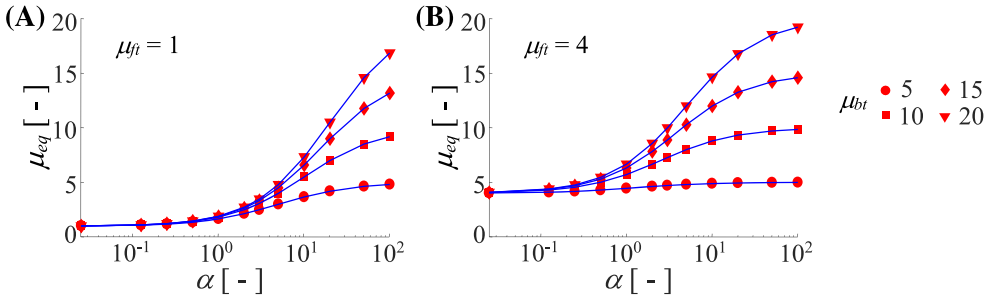

FIGURE 3 Equivalent ductility demand μ_{eq} of the dual system vs. base shear ratio α, for different values of μ_{ft} (1 and 4) and of μ_{bt} (5, 10, 15, and 20) [Colour figure can be viewed at wileyonlinelibrary.com]

are not included in the set. The large number of records considered allows the estimation, with good confidence, of the statistics of the response parameters, even of those commonly characterized by a significant dispersion such as the residual displacement.[36]

The seismic analyses are carried out with OpenSees.[49] The model of the SDOF dual system consists of two "truss" elements, arranged in parallel, fixed at one end, and connected to a mass at the other end. The nonlinear response of the two elements is described by the uniaxial elasto-plastic material models "Steel01" and "SteelBRB"[3,4] for the MRF and the BRBF, respectively. As previously explained, the model parameters of the "SteelBRB" material not involved in the parametric analysis are assumed equal to those in Zona and Dall'Asta[3] identified from the experimental tests by Tremblay et al.[5]

4.2 | Parametric study results

Figures 4 to 14 show the results of the parametric analysis. Plotted in each figure is the variation of a response parameter with the base shear ratio α obtained for different values of the BRBF's ductility demand μ_{bt} (i.e., 5, 10, 15, and 20). Different combinations of T_0 (i.e., 0.3, 1, and 2 s) and of the MRF's ductility demand μ_{ft} (i.e., 1 and 4) are also considered.

In order to facilitate the discussion of the results, it is worth reminding that, as demonstrated at the beginning of the section, increasing μ_{ft}, μ_{bt}, and α yields an increase of μ_{eq} and hence of the system nonlinearity. Moreover, it is worth mentioning that $\alpha = 0$ represents the case of the bare frame and hence, for $\alpha = 0$ the results are independent from the value of μ_{bt}. Similarly, $\alpha = 100$ corresponds to the frame with "pinned" connections where the horizontal stiffness and resistance is provided only by the BRBF. Hence, for $\alpha = 100$, the results are expected to be independent from μ_{ft}. It is important to highlight that the results of Figures 4 to 14 are plotted in a logarithmic scale for the α values and the first value plotted refers to $\alpha = 0.025$. The values for $\alpha = 0$ are numerically reported in the figures.

As mentioned before, the analyses were performed also for intermediate values of the parameters and a smooth transition of the results was observed while looking at intermediate values of μ_{ft} and T_0.

Figure 4 shows the geometric mean (GM) of the normalized peak displacement demand δ. Peak displacement (or drift) demand parameters are conventionally used as global EDPs for the assessment of building structures as they are strongly correlated with both structural and non-structural damage. The following observations can be made:

- All the curves, in each subplot, attain the same value of about 1 for $\alpha = 0$ and $\mu_{ft} = 1$. This result is expected, because for $\alpha = 0$ and for $\mu_{ft} = 1$, the system behaves (on average) elastically so that the inelastic displacement coincides with the elastic one;

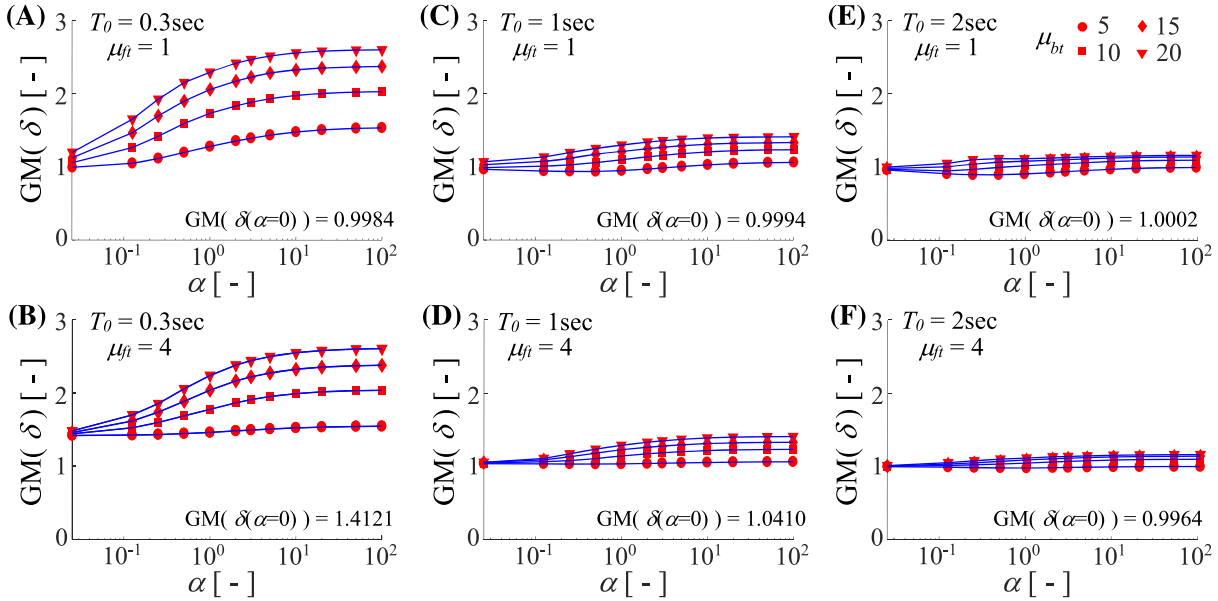

FIGURE 4 Geometric mean (GM) of the normalized peak displacement demand δ versus base shear ratio α, for different values of T_0 (0.3, 1, and 2 s), of μ_{ft} (1 and 4), and of μ_{bt} (5, 10, 15, and 20) [Colour figure can be viewed at wileyonlinelibrary.com]

- On the other hand, for $\alpha = 0$ and $\mu_{ft} = 4$, the nonlinear behavior of the MRF leads to values of δ significantly different than 1. In particular, for short periods structures (i.e., $T_0 = 0.3$ s), the normalized peak displacement δ attains values higher than 1;
- In the case of dual systems ($\alpha > 0$), the increase of α and/or of the BRBF's ductility demand μ_{bt} corresponds to an increase of the equivalent ductility demand μ_{eq} and hence, for short periods structures (i.e., $T_0 = 0.3$ s), of the normalized peak displacement δ;
- Differently, for higher periods (i.e., $T_0 = 2$ s), the normalized peak displacement δ is almost independent from the equivalent ductility demand μ_{eq} and attains values close to 1. Recalling that δ can be interpreted as the displacement amplification factor, these results are in agreement with the current state of knowledge reported in literature (i.e., equal energy and equal displacement rules).[50]

Figure 5 shows the dispersion β, expressed by the lognormal standard deviation, of the normalized peak displacement demand δ. The following observations can be made:

- The lowest dispersion values are observed for the systems corresponding to the elastic MRF only ($\alpha = 0$ and $\mu_{ft} = 1$), as expected;
- Overall, the dispersion increases for increasing μ_{eq} values, i.e., by increasing α, μ_{bt} and μ_{ft}, and for decreasing values of T_0;
- For $\mu_{ft} = 1$, the dispersion varies significantly with α, whereas for $\mu_{ft} = 4$, this variation is smaller, and this is related to the lower influence that α has on μ_{eq} for high μ_{ft} values (see Figure 3);
- For low values of T_0, the dispersion can attain values of the order of 0.7 in the case of BRBF only ($\alpha = 100$);
- The observed trends reflect the efficiency of the *IM* considered in this study (i.e., $S_a(\omega_0, \xi)$), which yields an almost null dispersion only in the case of $\alpha = 0$ and $\mu_{ft} = 1$, i.e. For inelastic systems, for the elastic bare frame. However, it is noteworthy to highlight that the dispersion is not exactly zero even for this case, because only the mean ductility demand is equal to 1, and thus, for some records, the system slightly exceeds the yielding force.

In is interesting to observe that both the normalized peak displacement demand δ (Figure 4) and its dispersion values (Figure 5) remain nearly constant for values of α larger than 3.

Figure 6 shows the time histories of u_{max} and δ under a single ground motion (i.e., record #100) for two design situations, corresponding to $T_0 = 0.3$ s, $\mu_{ft} = 1$, $\mu_{bt} = 20$ and α respectively equal to 0.025 and 3. It is possible to observe how the increase of α, and hence of the equivalent ductility demand μ_{eq}, yields to larger values of the normalized displacement demand δ. Differently, the time histories for the displacement demand u_{max} show how both cases attain the same

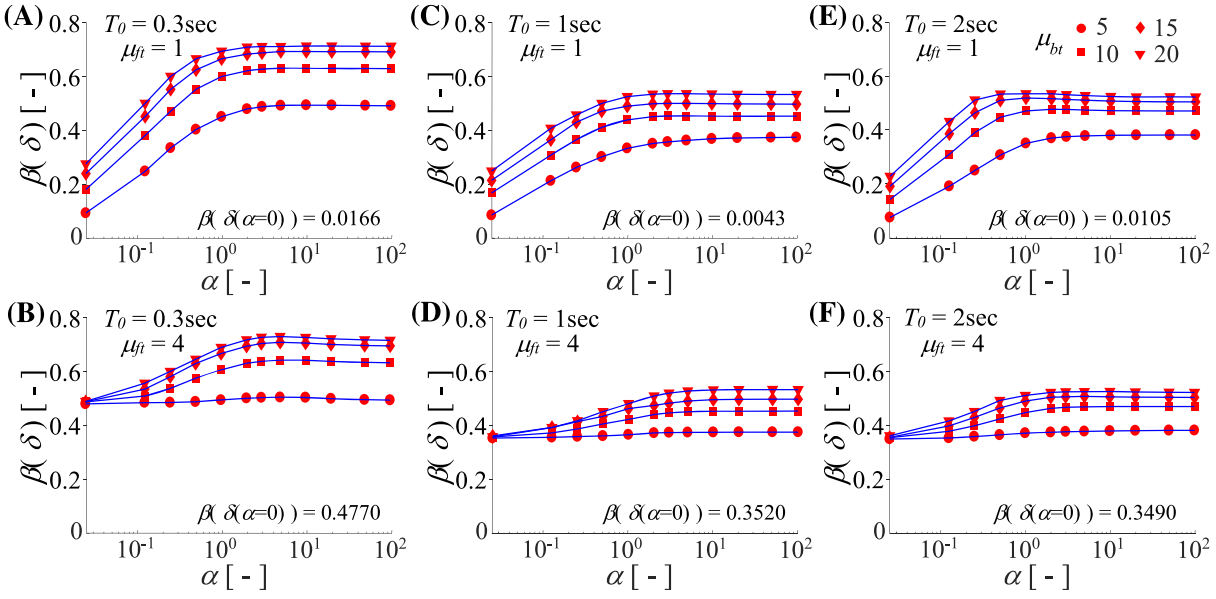

FIGURE 5 Dispersion of the normalized peak displacement demand δ versus base shear ratio α, for different values of T_0 (0.3, 1, and 2 s), of μ_{ft} (1 and 4), and of μ_{bt} (5, 10, 15, and 20) [Colour figure can be viewed at wileyonlinelibrary.com]

maximum displacement value equal to about 1. This offers the opportunity to remind the reader that, in order to use the nondimensional parameters, for each system of the parametric analysis, the ground motions are scaled in order to attain the design condition. This is attained when the mean values of the peak displacement demand $\bar{u}_{max,t} = 1$ m under the set of records (the results of the parametric analysis are independent from the choice of this value given that the structural properties are defined as a function of $\bar{u}_{max,t}$).

Figure 7 shows the GM of the normalized peak absolute acceleration α_{abs}. This demand parameter is conventionally used as EDP to assess the seismic performance of acceleration-sensitive nonstructural components (e.g., mechanical equipment and elevators) and building contents. The following observations can be made:

- As can be expected, α_{abs} is about equal to 1 for the systems corresponding to the elastic MRF only ($\mu_{ft} = 1$ and $\alpha = 0$) and reduces by increasing μ_{eq} (i.e., by increasing the values of α, of μ_{bt} and of μ_{ft});
- For inelastic systems, i.e., μ_{ft} ? 1 and/or $\alpha > 0$, α_{abs} slightly increases as T_0 decreases;
- For $\mu_{ft} = 1$, the value of α_{abs} varies significantly with α. On the other hand, for increasing values of μ_{ft} this variation becomes less significant and, in the cases with $\mu_{ft} = 4$, α_{abs} is almost independent of α. However, even for the case of elastic MRF ($\mu_{ft} = 1$), α_{abs} does not decrease significantly for values of α increasing beyond 1;
- The results show that an increase of μ_{bt} leads to an about consistent reduction of α_{abs} independently from the structural periods T_0 and MRF's ductility demand μ_{ft}. A similar outcome but opposite in terms of variation is observed in Figure 4 while considering the variation of normalized peak displacement demand δ.

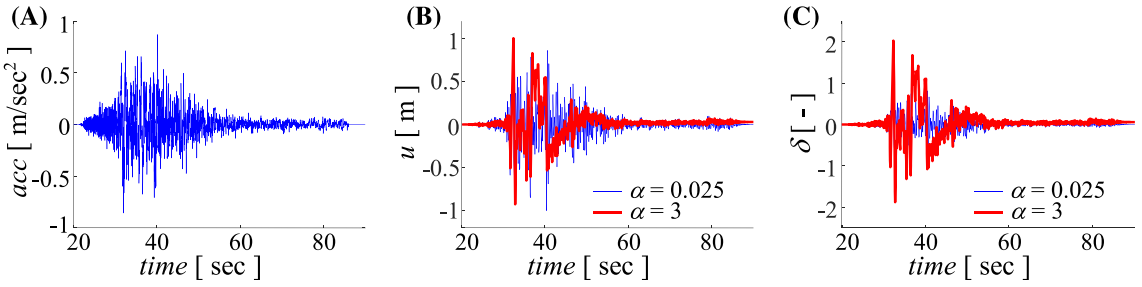

FIGURE 6 Seismic response of systems with $T_0 = 0.3$ s, $\mu_{ft} = 1$, $\mu_{bt} = 20$, and $\alpha = 0.025$ and 3. A, Seismic record #100, B, peak displacement demand u_{max} at the design condition, and C, normalized peak displacement demand δ [Colour figure can be viewed at wileyonlinelibrary.com]

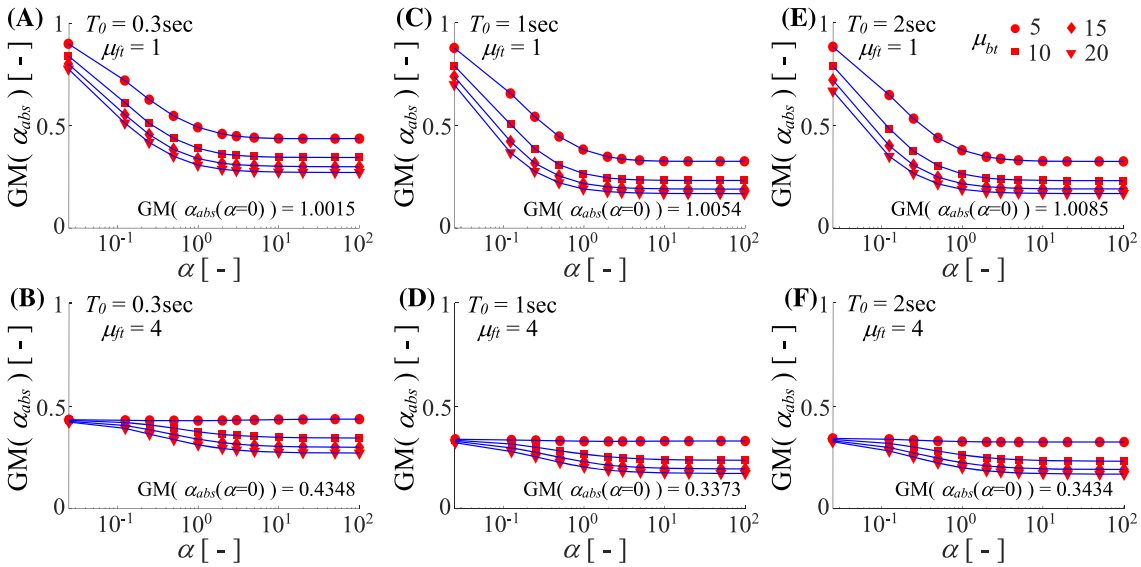

FIGURE 7 Geometric mean (GM) of the normalized peak absolute accelerations demand α_{abs} versus base shear ratio α, for different values of T_0 (0.3, 1, and 2 s), of μ_{ft} (1 and 4), and of μ_{bt} (5, 10, 15, and 20) [Colour figure can be viewed at wileyonlinelibrary.com]

Figure 8 shows the dispersion β of the normalized peak absolute acceleration α_{abs}. In general, the values of β are quite low and always below 0.3. This is a consequence of the yielding of the system that limits the maximum accelerations that can be attained. The following observations can be made:

- Also in this case, the lowest dispersion values are observed for the systems corresponding to the elastic MRF ($\alpha = 0$ and $\mu_{ft} = 1$), and as previously discussed, the dispersion is not exactly zero even for this case, because the design procedure impose a ductility demand is equal to 1 only on average;
- In all cases, the dispersion increases for increasing values of μ_{bt} whereas an increase of the MRF's ductility demand μ_{ft} yields a reduction of the dispersion;
- For the cases with an elastic MRF (i.e., $\mu_{ft} = 1$), a larger variation of the dispersion values with α can be noted, whereas for $\mu_{ft} = 4$, this variation is smaller. In addition, different from what observed in the dispersion of the normalized displacement demand δ (Figure 5), where the trends are consistent, the use of an elastic MRF (i.e., $\mu_{ft} = 1$) leads to higher dispersion values within the range of α between 0 and 1. The obtained results show a maximum dispersion value equal to 0.3 for the case with $\mu_{ft} = 1$, $\mu_{bt} = 20$ and $\alpha = 0.25$.

Also in this case, it is interesting to observe that both the normalized peak absolute acceleration α_{abs} (Figure 7) and its dispersion values (Figure 8) remain almost constant for values of α larger than 3.

Figure 9 shows the time histories of a_{max} and α_{abs} under a single ground motion (i.e., record #100) for two design situations. Two cases are represented, corresponding to $T_0 = 0.3$ s, $\mu_{ft} = 1$, $\mu_{bt} = 20$ and α respectively equal to 0.025 and 3. It is observed that increasing α, and hence, the equivalent ductility demand μ_{eq}, yields to lower values of the normalized acceleration demand α_{abs}.

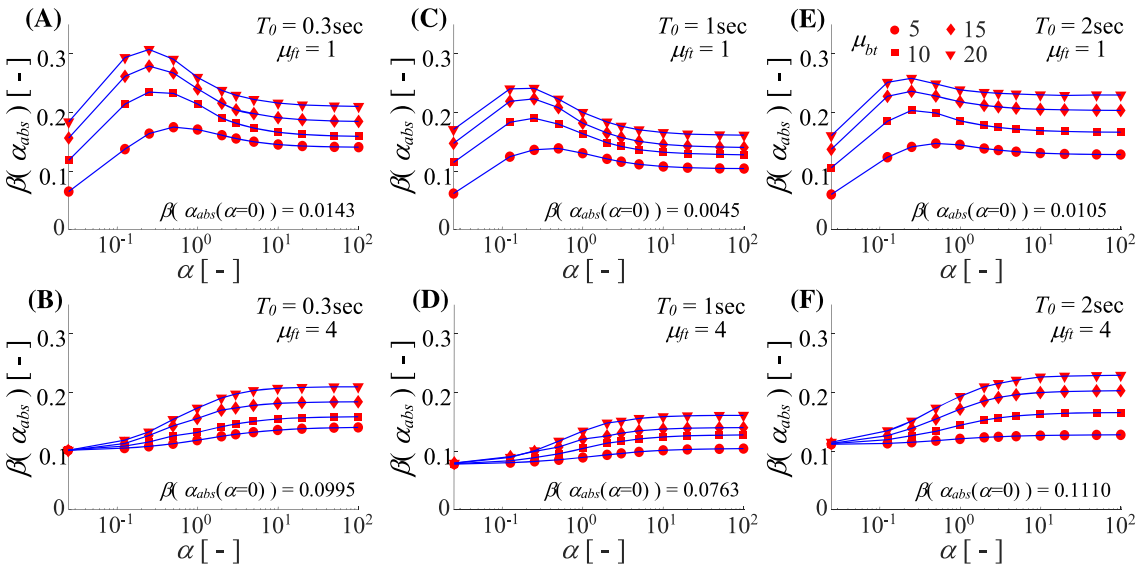

FIGURE 8 Dispersion of the normalized peak absolute accelerations demand α_{abs} versus base shear ratio α, for different values of T_0 (0.3, 1, and 2 s), of μ_{ft} (1 and 4), and of μ_{bt} (5, 10, 15, and 20) [Colour figure can be viewed at wileyonlinelibrary.com]

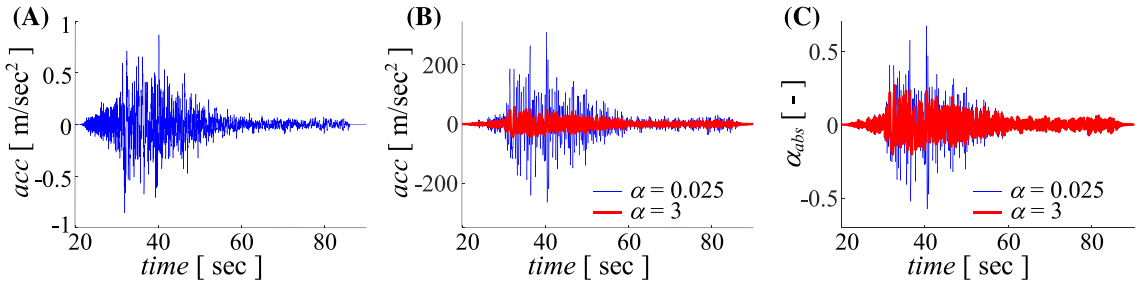

FIGURE 9 Seismic response of systems with $T_0 = 0.3$ s, $\mu_{\text{ft}} = 1$, $\mu_{bt} = 20$, and $\alpha = 0.025$ and 3. A, Seismic record #100, B, peak acceleration demand, and C, normalized peak acceleration demand α_{abs} [Colour figure can be viewed at wileyonlinelibrary.com]

Figure 10 shows the GM of the BRBF's normalized cumulative ductility demand $\mu_{b,cum}$. This is also an important response parameter that controls not only the isotropic hardening of the BRB[3] but also its failure, as acknowledged in several capacity models of these devices.[10,11] The following observations can be made:

- For this parameter, values for the systems with $\alpha = 0$ are not reported because this corresponds to the case of MRF only;
- In the case of dual systems (i.e., $\alpha > 0$), the increase of α, of the BRBF's ductility demand μ_{bt} and/or of the MRF's ductility demand μ_{ft} corresponds to an increase of the equivalent ductility demand μ_{eq} resulting in fewer cycles at the maximum deformation and a smaller BRBF's ductility accumulation;
- This effect is clearly reported in Figure 6 where the seismic response of the system with $\alpha = 3$ shows a significant lower number of cycles with large displacements with respect to the case with $\alpha = 0.025$.
- The observed trends suggest that higher α values permit a better control of the cumulative ductility demand in the BRBFs. However, the decrease is higher for low α values, whereas for $\alpha > 3$, the cumulative ductility does not decrease significantly, similar to the normalized peak absolute accelerations demand α_{abs} of Figure 7;
- A high sensitivity of the parameter $\mu_{b,cum}$ with respect to α is observed only for the case with elastic MRF (i.e., $\mu_{ft} = 1$) and short period structures (i.e., $T_0 = 0.3$ s). For higher periods (i.e., $T_0 = 2$ s), the BRBF's normalized cumulative ductility demand is almost independent from α;
- The highest value of the BRBF's normalized cumulative ductility demand $\mu_{b,cum}$ reaches the value of about 800 in the case with elastic MRF (i.e., $\mu_{ft} = 1$), highly ductile BRBF (i.e., $\mu_{bt} = 20$) and small α values;
- This value is about half in the case with $\mu_{ft} = 4$ where the inelastic MRF contributes to the seismic dissipation capacity of the system with plastic deformations that are not accumulated in the devices;
- Moreover, as expected, the results show that an increase of the BRBF's ductility demand μ_{bt} leads to a consistent increase of the value $\mu_{b,cum}$ independently from the structural periods T_0 and MRF's ductility demand μ_{ft}. This outcome is similar to what observed in Figure 4 for the variation of normalized peak displacement demand δ;
- These trends are in agreement with the results obtained in Choi and Kim,[34] which investigated the case of BRBF only (i.e., $\alpha = 100$).

Figure 11 shows the dispersion β of the BRBF's normalized cumulative ductility demand $\mu_{b,cum}$. In general, the values of β are quite high, and can reach a maximum of 0.65. This reflects the variation of duration of the considered records. Overall, the dispersion does not significantly change with the period, with μ_{ft}, and with μ_{bt}, and in most of the cases is slightly increases for increasing α values.

Beside the dispersion values, it is interesting to observe that, similarly to the previous cases, also the BRBF's normalized cumulative ductility demand $\mu_{b,cum}$ (Figure 10) and its dispersion values (Figure 11), remain almost constant for

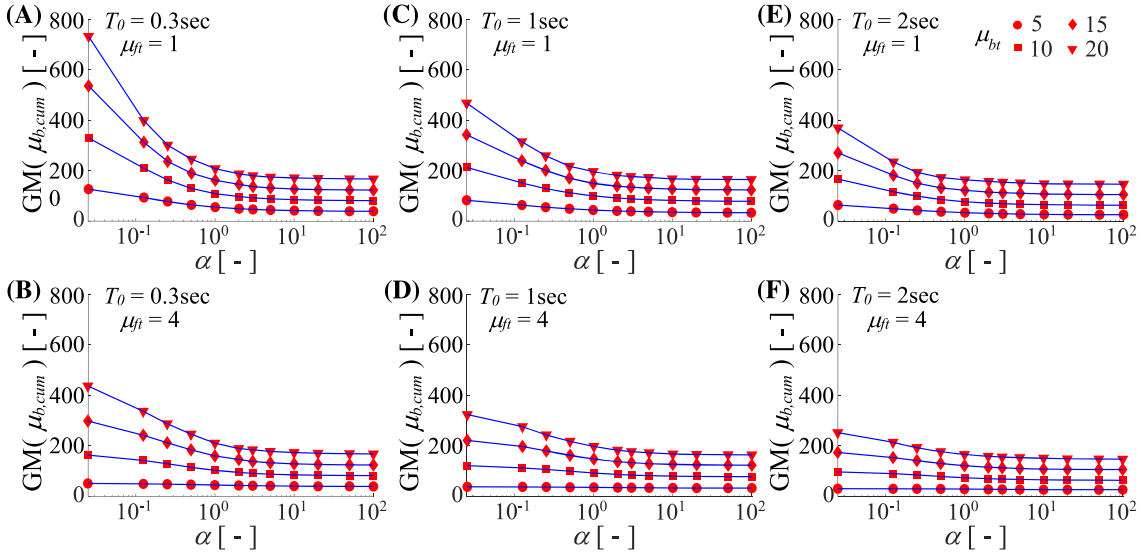

FIGURE 10 Geometric mean (GM) of the BRBF's normalized cumulative ductility demand $\mu_{b,cum}$ versus base shear ratio α, for different values of T_0 (0.3, 1, and 2 s), of μ_{ft} (1 and 4), and of μ_{bt} (5, 10, 15, and 20) [Colour figure can be viewed at wileyonlinelibrary.com]

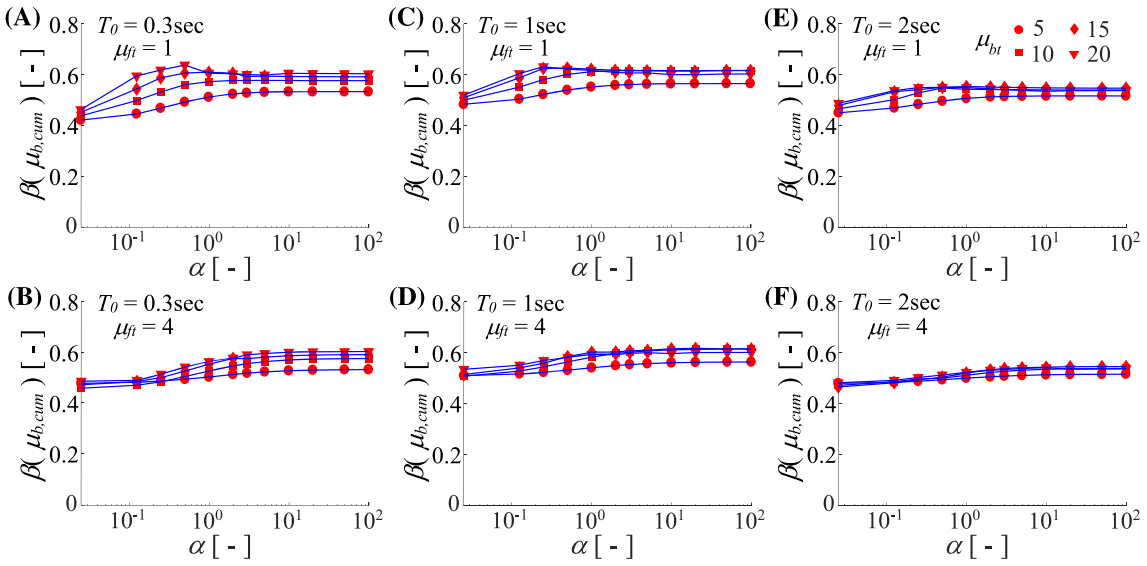

FIGURE 11 Dispersion of the BRBF normalized cumulative ductility demand $\mu_{b,cum}$ versus base shear ratio α, for different values of T_0 (0.3, 1, and 2 s), of μ_{ft} (1 and 4), and of μ_{bt} (5, 10, 15, and 20) [Colour figure can be viewed at wileyonlinelibrary.com]

values of α larger than 3. This result, observed also for the parameters δ and α_{abs}, justifies the limit posed by SEI/ASCE 7-10[26] on the maximum values of $\alpha = 3$ in dual systems. In fact, based on the results for the parameters δ, α_{abs}, and $\mu_{b,cum}$, the influence of the MRF within the dual system is negligible for α values larger than 3.

Figure 12 shows the time history of μ_{cum} and $\mu_{b,cum}$ under a single ground motion (i.e., record #100) for the two design situations corresponding to $T_0 = 0.3$ secs, $\mu_{ft} = 1$, $\mu_{bt} = 20$ and α respectively equal to 0.025 and 3. The consequence of the different displacement history, i.e., lower number of cycles with large displacements for the system with $\alpha = 3$, observed in Figure 6, and summarized in Figure 10, can be clearly observed in this figure.

Figure 13 shows the GM of the normalized residual displacement demand δ_{res}. As previously discussed, this response parameter is related to building reparability. The following observations can be made:

- All the curves, in each subplot, attain the same value of about 0 for $\alpha = 0$ and $\mu_{ft} = 1$. This result is expected, because this case corresponds to the elastic MRF only. On the other hand, for $\alpha = 0$ and $\mu_{ft} = 4$, the nonlinear behavior of the MRF leads to δ_{res} values that can be significantly different than 0;
- Overall, the normalized residual displacement demand δ_{res} increases for increasing μ_{eq} (i.e., for increasing values of α, of μ_{bt}, and of μ_{ft}) and is almost independent from T_0;
- In the case of elastic MRFs (i.e., $\mu_{ft} = 1$), the variation of α significantly affects the increase of the residual displacements δ_{res}, whereas this parameter is almost constant with α in the case of systems with ductile MRF (i.e., $\mu_{ft} = 4$). The elastic MRF works, within the dual system, as a back-up frame and this has a beneficial contribution in terms of reduction of δ_{res}. This result confirms the effectiveness of coupling a dissipative system with an elastic system as a way to reduce residual drifts;

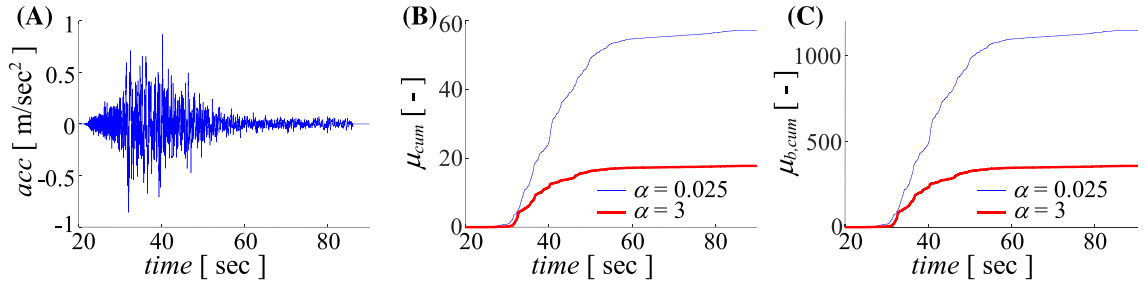

FIGURE 12 Seismic response of systems with $T_0 = 0.3$ s, $\mu_{ft} = 1$, $\mu_{bt} = 20$, and $\alpha = 0.025$ and 3. A, Seismic record #100, B, BRBF's cumulative ductility demand, and C, BRBF's normalized cumulative ductility demand $\mu_{b,cum}$ [Colour figure can be viewed at wileyonlinelibrary.com]

- Amongst all the analyzed cases, the normalized residual displacement demand δ_{res} assumes maximum values of the order of 0.3. It is noteworthy that the values of δ_{res} for $\alpha = 0$ and $\mu_{ft} = 4$ are similar to the ones observed in Liossatou and Fardis[51] for an elasto-plastic system with a strength reduction factor of 4 under a different set of records than the one considered in this study.

Figure 14 shows the dispersion β of the normalized residual displacement demand δ_{res}. These values are very high, especially for low values of the MRF ductility demand and low values of α.

Among others, for this response parameter, and differently from the others, it is interesting to observe that, in the case of an elastic MRFs (i.e., $\mu_{ft} = 1$), the variation of α significantly affects the results also for α values larger than

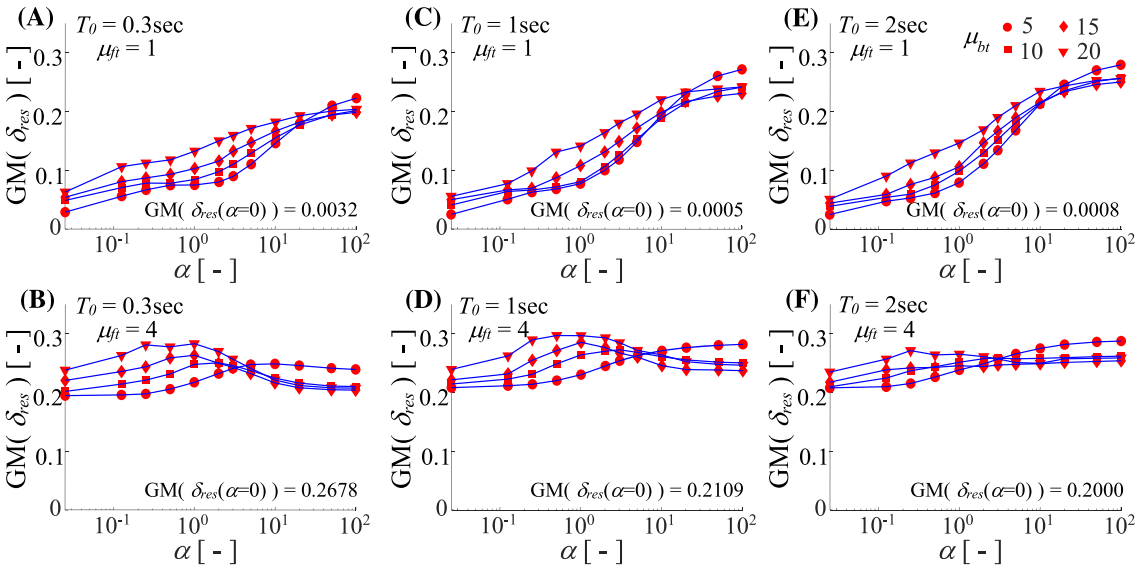

FIGURE 13 Geometric mean (GM) of the normalized residual displacement demand δ_{res} versus base shear ratio α, for different values of T_0 (0.3, 1, and 2 s), of μ_{ft} (1 and 4), and of μ_{bt} (5, 10, 15, and 20) [Colour figure can be viewed at wileyonlinelibrary.com]

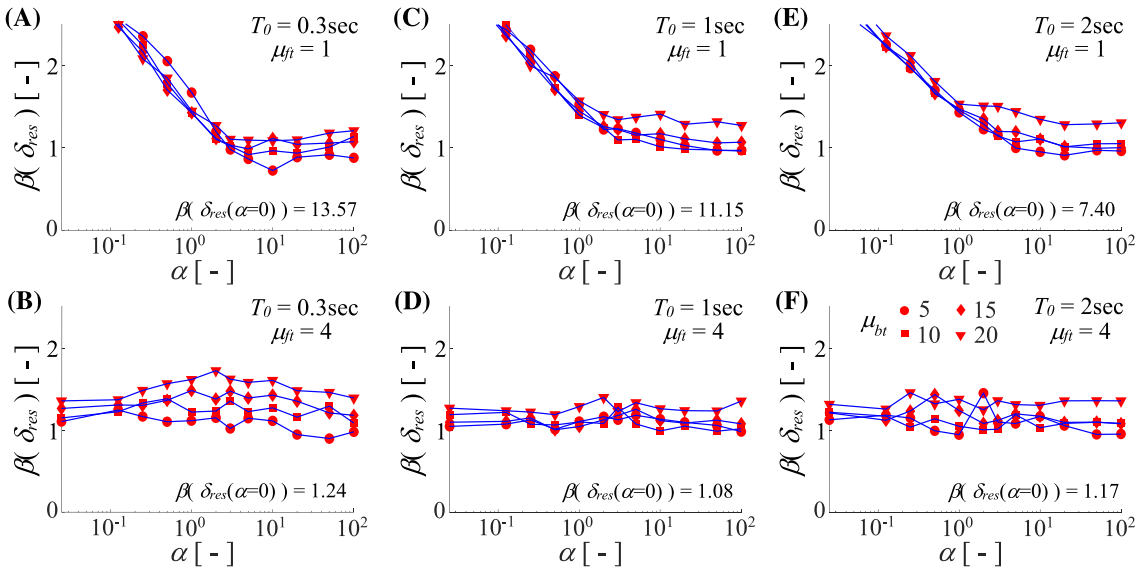

FIGURE 14 Dispersion of the normalized residual displacement demand δ_{res} versus base shear ratio α, for different values of T_0 (0.3, 1, and 2 s), of μ_{ft} (1 and 4), and of μ_{bt} (5, 10, 15, and 20) [Colour figure can be viewed at wileyonlinelibrary.com]

3. This result has significant implications when controlling the residual displacements is a required design objective in order to allow reparability and achieve structural resilience.

It is worth mentioning that the parametric analyses were repeated also using other ground motion sets such as the SIMBAD database[52] and the far-fault records of the FEMA P695 project,[53] leading to only slightly different results, thus confirming the overall trend of variation of the dispersion values with respect to the nondimensional parameters analyzed. Moreover, the obtained estimates may change significantly by using a different constitutive law for describing the hysteretic response of the SDOF system representing the frame (see, e.g., Guerrero et al[31] and Liossatou and Fardis[51]).

5 | COMPARISONS WITH MDOF RESULTS

The generality and the limitations of the results obtained by considering an SDOF system are evaluated by considering two realistic dual systems structures, modeled as multi-degrees of freedom (MDOF) systems. The first case consists of a newly designed three-story dual steel MRF with BRBs, where the MRF is designed to remain elastic at the design condition. This corresponds to a target ductility of the MRF $\mu_{ft} = 1$, as controlled by the top story displacement (TSD) (i.e., control node in the pushover analysis). The second case consists of an existing three-story RC MRF retrofitted with BRBs. In this case, the MRF is allowed to undergo inelastic deformations and the target ductility is assumed equal to $\mu_{ft} = 4$. This corresponds to a situation where the MRF experiences large deformations beyond its elastic limit and is close to the collapse condition.

Three values of the base shear ratio α are considered for each case study, i.e., 0.1, 1, and 3 for the dual steel MRF with BRBs and 0.1, 0.5, and 1 for the RC MRF retrofitted with BRBs. High values of α in the RC MRF retrofitted with BRBs may require the introduction of local strengthening of beams and columns in the bays of the frame where the BRBs are installed,[8] interventions excluded in the cases analyzed in this study. Different from what is done in the parametric analysis of the SDOF systems, in this part of the study, the MRFs are kept constant, and the different α values are obtained by increasing the BRBs dimensions. This leads to an increase of the overall stiffness of the system, hence, in a reduction of the natural period.

The design of the dissipative braces follows the procedure described in Freddi et al,[8] where the stiffness and strength of the dissipative brace components, i.e., elastic brace and dissipative device, are calibrated according to the first mode-shape with the aim of achieving the simultaneous yielding of the BRB devices at various stories. This condition is usually sought in the design because it maximizes the dissipation capacities of the system. Additional details on the design procedure can be found in the literature.[7,8,33] Strength, F_b, stiffness, K_b, and ductility, μ_b, of the dissipative brace are function of the properties of the two components according to the following relationships:

$$F_b = F_0,\ K_b = \frac{K_0 K_{eb}}{K_0 + K_{eb}},\ \mu_b = \frac{K_0 + K_{eb}\mu_0}{K_0 + K_{eb}}, \tag{9}$$

where F_0, K_0, and μ_0 are respectively the yielding force, the stiffness, and the ductility capacity of the BRB device whereas K_{eb} is the stiffness of the elastic brace. Obviously, the elastic brace must be designed such that the yielding and buckling resistance is higher than F_0.

In both the cases, the ductility capacity of the BRB device μ_0 is assumed equal to 20 whereas the ductility of the dissipative brace μ_b is chosen equal to 10 and 15 respectively for the cases of newly designed dual steel MRF and existing RC MRF. The target values for the ductility of the dissipative brace μ_b can be obtained by the proper design of the elastic brace placed in series with the BRB device according to Equation 9. The analyses performed on the MDOF systems follow the same approach used for the SDOF where the ground motion records are scaled in an iterative way until the design condition is attained.

5.1 | Newly designed dual steel MRF and BRBF

The first case is a three-story six-bay by four-bay dual system composed by a steel MRF and a BRBF. The building has a constant inter-story height of 3.5 m, a total height of 10.5 m, and plan dimensions of 39 m by 26 m respectively along the x and y directions. Figure 15 shows the plan and elevation views of the building. For both the directions, the

horizontal actions are resisted by two perimeter MRFs and by two internal BRBFs. The design basis earthquake, with a probability of exceedance of 10% in 50 years, is expressed by the type 1 elastic response spectrum of Eurocode 8[15] with peak ground acceleration equal to 0.306 g and ground type C. The gravity loads and the live loads are assumed as uniformly distributed and assume values respectively of $G = 5.4$ kN/m^2 and $q_k = 3$ kN/m^2. The gravity loads are transferred directly to the beams lying in the orthogonal direction due to the presence of a one-way slab, which runs parallel to the direction of the seismic action. The total mass of the building is equal to 325.6 tons at each story. In this case, the MRF is designed to behave elastically up to a performance displacement of the top story equal to 0.105 m, which corresponds to a top floor drift of 1%. Both beams and columns are made with steel S355 (yield stress $f_y = 355$ MPa) and the design leads to the sections' dimensions reported in Figure 15. It is worth mentioning that, although designed to meet the Eurocode 8 prescriptions, US W-type sections instead of European sections were used for the steel MRF in order to simplify the design procedures, as commented in Maley et al.[23]

Given the symmetry of the structure and of the loading condition, only half of the structure comprising one dual system is analyzed, by developing a two-dimensional FE model in OpenSees.[49] Columns of the MRF are modeled by a distributed plasticity approach by using "nonlinearBeamColumn" elements[49] where the bilinear elastoplastic material "Steel01" with yield strength equal to 355 MPa and strain hardening of 0.2% is assigned to the steel fibers. Differently, beams are modeled through a lumped plasticity approach where the plastic hinges at beams ends are modeled by "zeroLength" rotational springs. Such springs are characterized by the degrading modified Ibarra-Medina-Krawinkler hysteretic bilinear model.[54,55] Stiffness matrices of the elastic elements between plastic hinges are modified through the "n" modification factor[56] allowing for the use of initial stiffness proportional Rayleigh damping, with 3% of the critical damping assigned to the first and second modes. MRF panel zones are modeled using the Scissors approach[57] where two independent rotational springs modeled as "zeroLength" elements are used to account for the deformability of columns' webs and flanges. On the other side, the BRBF is described using "elasticBeamColumn" elements with negligible inertia for beams and columns in order to reproduce pinned connections. The dissipative braces are modeled by two "truss" elements in series to represent respectively the elastic component of the brace and the BRB device. As for the case of the SDOF system, the "steelBRB" material model[3,4] describes the hysteretic behavior of the BRB devices, with the model parameters assumed equal to those reported in Zona and Dall'Asta[3] and identified from the tests described in Tremblay et al.[5] P-Δ effects are taken into account by modeling the gravity columns with an equivalent continuous lean-on column, pinned at its base, as described in Freddi et al.[58] Finally, diaphragm action is accounted by means of rigid truss elements connecting the nodes of the lean-on column to the ones of the beams of the MRF and of the BRBF. A similar dual frame configuration was studied in Morfuni et al,[59] who investigated the seismic behavior of an eight-story building structure.

The structural period of the MRF alone is equal to $T_1 = 1.80$ s. After adding the BRBF, the structural period decreases to 1.28, 0.55, and 0.33 s, respectively, for $\alpha = 0.1$, 1, and 3. Figure 16 shows the pushover curves for the three design conditions, exhibiting different proportion of the base shear (V_b) between the MRF and the BRBs.

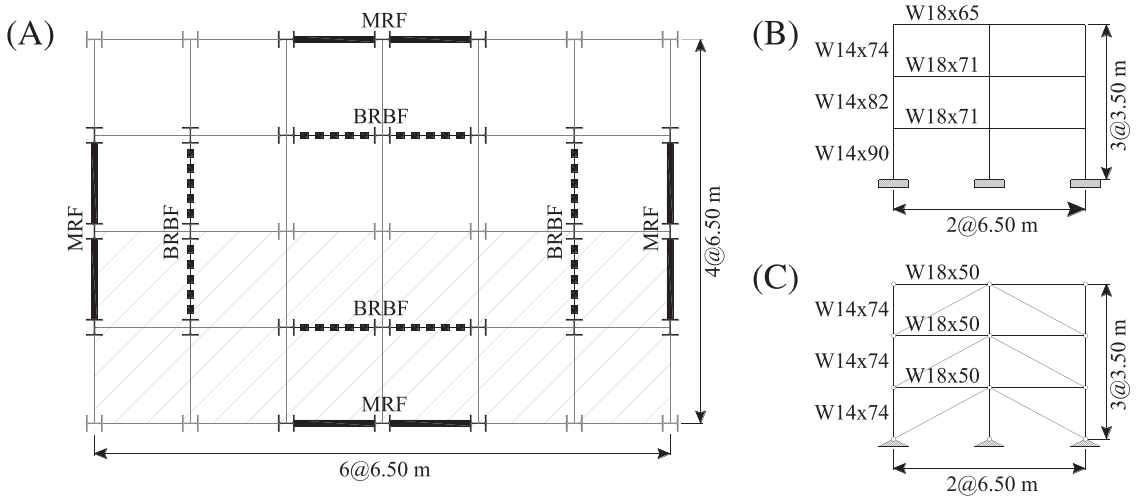

FIGURE 15 Newly designed dual steel MRF and BRBF. A, Plan view, B, elevation view of the MRFs, and C, elevation view of the BRBFs

5.2 | RC MRF retrofitted with BRBs

The second case consists in a three-story four-bay by three-bay ordinary RC MRF that was already considered in previous works by the authors.[8,35] This structure was chosen because an extended experimental campaign was carried out on a 1:3 reduced scale models of the frame and of its subassemblies, allowing an accurate validation of the FE model at global and local scale.[60] The building was designed for gravity loads only and without any seismic detailing, by applying the design rules existing before the introduction of modern seismic codes. The frame has an inter-story height of 3.66 m, for a total height of 11 m, and three bays each 5.49 m wide. Columns have a 300 × 300 mm^2 square section, whereas beams are 230 × 460 mm^2 at each floor. Grade 40 steel (f_y = 276 MPa) and concrete with compression resistance f_c = 24 MPa were employed in the design. Because earthquake loads were neglected and wind induced forces on such a low-rise structure were relatively small, no lateral load was considered for the design. Figure 17 shows the elevation view and sections of the RC frame. Complete detailing regarding the structure and the experimental campaign can be found in Bracci et al.[60]

A two-dimensional FE model of the structure was developed in OpenSees[49] and validated against experimental results (see Freddi et al[8,35]). The model employed in the present study is an enhanced version that employs the Zona et al[3] model for describing the BRBs. The design of the dissipative braces follows the same procedure described in the previous section.

As discussed, the design displacement of the coupled system is such that the ductility demand on the MRF μ_{ft} is equal to 4. This value is derived after bi-linearization of the capacity curve as reported in Figure 18. In the present case, the design displacement corresponds to a top story displacement equal to 0.339 m, i.e., a drift of 3.1%.

The structural period of the MRF alone is equal to T_1 = 1.28 s whereas, when adding the BRBF working in parallel, the structural period decreases and is equal to 1.10, 0.79, and 0.64 s, respectively, for α equal to 0.1, 0.5, and 1. Figure 18 shows the pushover curves for the three design conditions with the different contributions of the base shear (V_b) from the MRF and the BRBs.

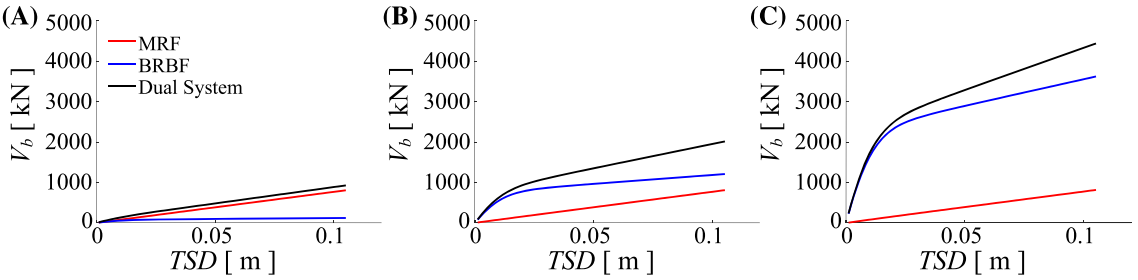

FIGURE 16 Newly designed dual steel MRF and BRBF. Pushover curves for α equal to A, 0.1, B, 1, and C, 3 [Colour figure can be viewed at wileyonlinelibrary.com] [Colour figure can be viewed at wileyonlinelibrary.com]

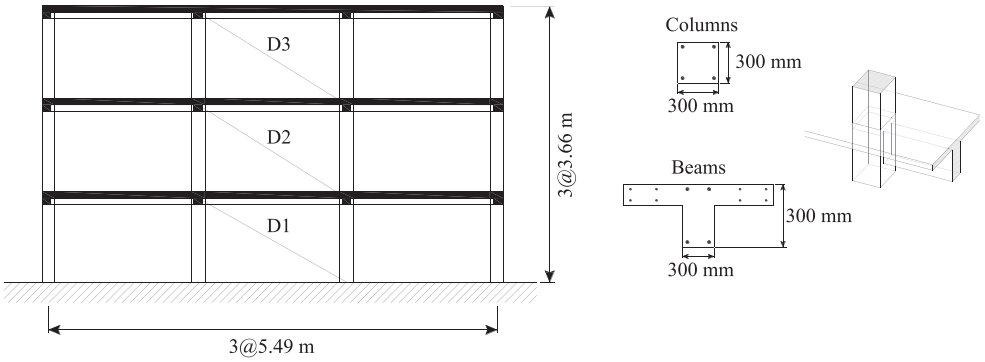

FIGURE 17 Seismic retrofitting of the RC MRF with BRBs. Elevation view

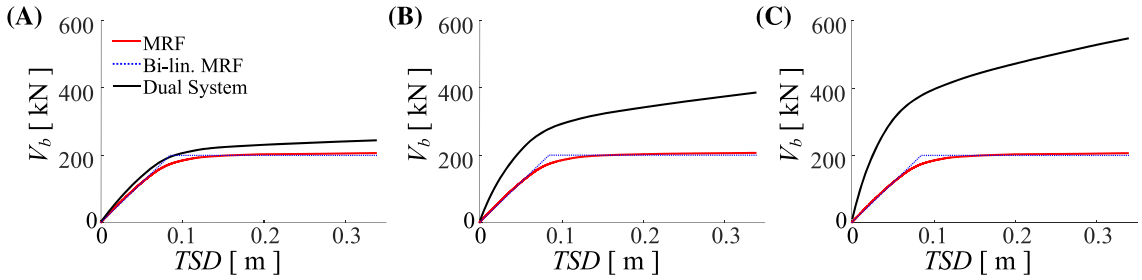

FIGURE 18 Seismic retrofitting of the RC MRF with BRBs. Pushover curves for α equal to A, 0.1, B, 0.5, and C, 1 [Colour figure can be viewed at wileyonlinelibrary.com] [Colour figure can be viewed at wileyonlinelibrary.com]

5.3 | Comparison of the results

Figures 19 to 22 compare the results obtained with the MDOF systems to the corresponding results obtained using the SDOF system approximation. In particular, Figures 19 and 21 show the variation with α and T_0 of the GM of the four nondimensional response parameters of interest, whereas Figures 20 and 22 show the variation of their dispersion. The values reported for the MDOF cases are the maximum ones observed throughout the system height. Tables 1 and 2 reports the values of the median and dispersion of the parameters according to the MDOF and SDOF model respectively for the newly designed dual steel MRF and BRBF and for the RC MRF retrofitted with BRBs. The results for the SDOF case are obtained by linear interpolation of the values obtained in the parametric study.

It can be observed that the results of the two MDOF systems follow trends similar to those obtained with the simplified SDOF models, with few exceptions. The observed differences are mainly due to (1) the influence of higher modes of vibration not accounted by the SDOF systems and (2) the simplified description of the post-elastic hysteretic behavior of the MRF in the SDOF models. Higher discrepancies are expected for taller structures due to the increment of the effects of higher modes, and for the frames that undergo significant inelastic deformations, due to the inevitable differences between the hysteretic behavior of the MDOF and SDOF models. The effect of higher modes can be observed in Figures 19B and 21B, showing that the normalized peak absolute acceleration demand is significantly underestimated by the SDOF model. Differently, the simplified description adopted for the hysteretic behavior of the SDOF system affects only the response estimates obtained for the retrofitted RC frame, because the steel MRF behaves almost elastically.

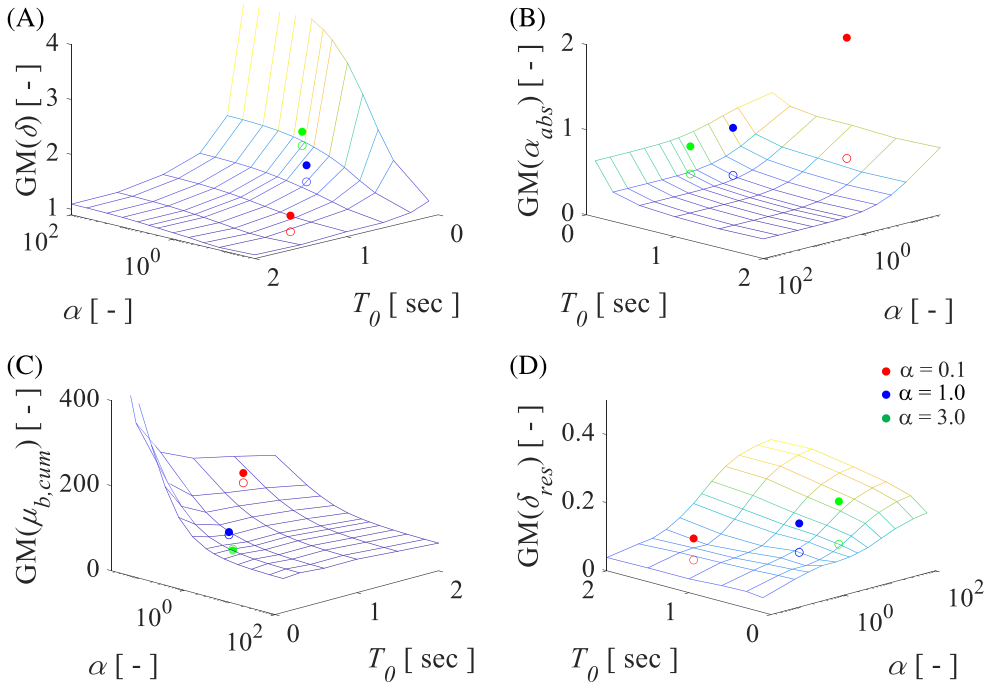

FIGURE 19 Newly designed dual steel MRF and BRBF. Comparison of the parametric analyses for SDOF and MDOF. Geometric mean (GM) of the A, normalized peak displacement demand δ, B, normalized peak absolute accelerations demand α_{abs}, C, BRBF's normalized cumulative ductility demand $\mu_{b,cum}$, D, normalized residual displacement demand δ_{res} versus base shear ratio α, for different values of T_0 and of $\mu_{ft} = 1$ and $\mu_{bt} = 10$ [Colour figure can be viewed at wileyonlinelibrary.com]

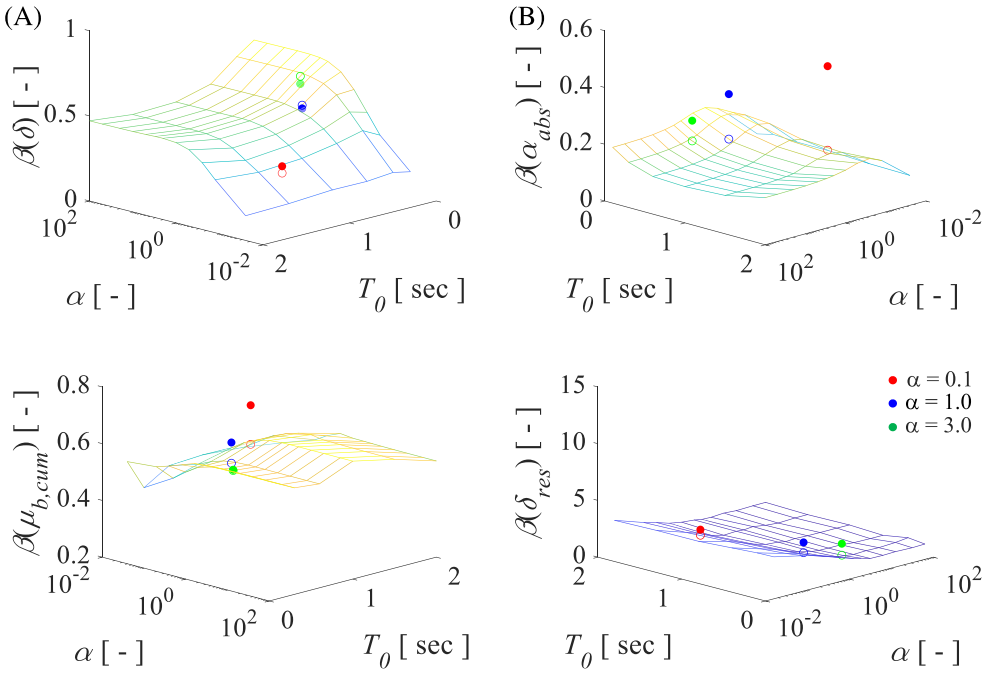

FIGURE 20 Newly designed dual steel MRF and BRBF. Comparison of the parametric analyses for SDOF and MDOF. Dispersion of the A, normalized peak displacement demand δ, B, normalized peak absolute accelerations demand α_{abs}, C, BRBF's normalized cumulative ductility demand $\mu_{b,cum}$, D, normalized residual displacement demand δ_{res} versus base shear ratio α, for different values of T_0 and of $\mu_{ft} = 1$ and $\mu_{bt} = 10$ [Colour figure can be viewed at wileyonlinelibrary.com]

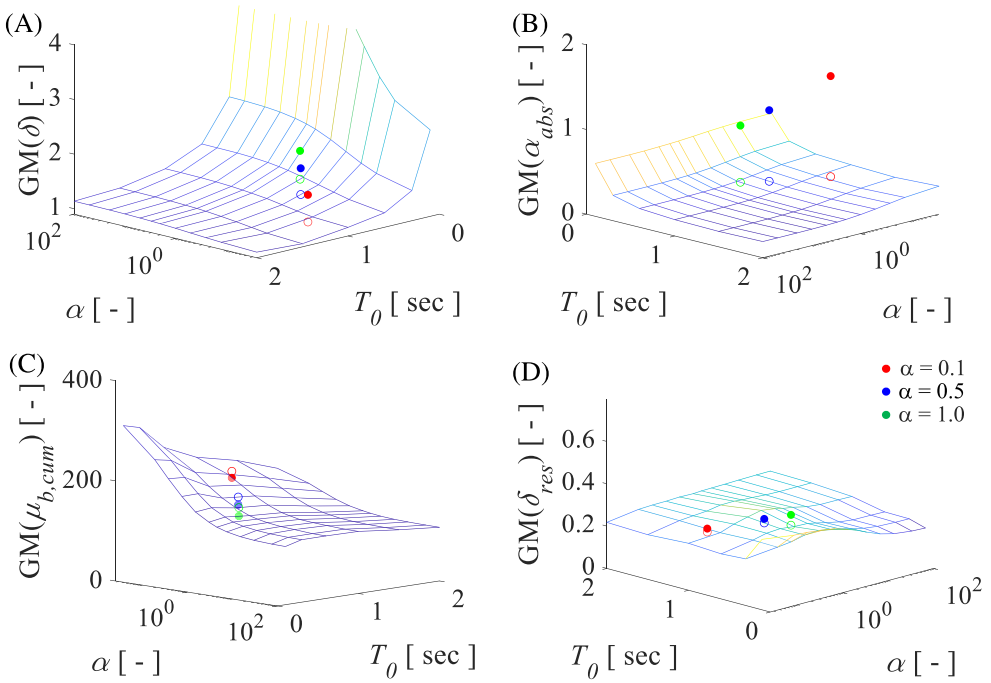

FIGURE 21 Seismic retrofitting of a RC MRF with BRBs. Comparison of the parametric analyses for SDOF and MDOF. Geometric mean (GM) of the A, normalized peak displacement demand δ, B, normalized peak absolute accelerations demand α_{abs}, C, BRBF's normalized cumulative ductility demand $\mu_{b,cum}$, D, normalized residual displacement demand δ_{res} versus base shear ratio α, for different values of T_0 and of $\mu_{ft} = 4$ and $\mu_{bt} = 15$ [Colour figure can be viewed at wileyonlinelibrary.com]

Tables 1 and 2 report also the relative differences between the estimates obtained with the SDOF model and the MDOF model, normalized by dividing them by the values obtained with the SDOF model. Based on the obtained results, for the newly designed dual steel MRF and BRBF, the following consideration can be made: (i) for the GM of the normalized peak displacement demand δ, the differences in the three cases range between 14% and 31%; (ii) for the GM of the normalized peak absolute accelerations demand α_{abs}, the values obtained with the MDOF model can be more than double the SDOF model; (iii) for the GM of the BRBF's normalized cumulative ductility demand $\mu_{b,cum}$, the values obtained with the SDOF and MDOF models are much closer, with differences spanning from 4 to 15%; (iv) for the GM of the normalized residual displacement demand δ_{res}, the MDOF models yield values that are about twice as those of the SDOF models. Similar considerations can be made for case of the RC frame retrofitted with BRBs, with some exceptions. In particular, compared with the results of Tables 1, the influence of the nonlinear behavior of the

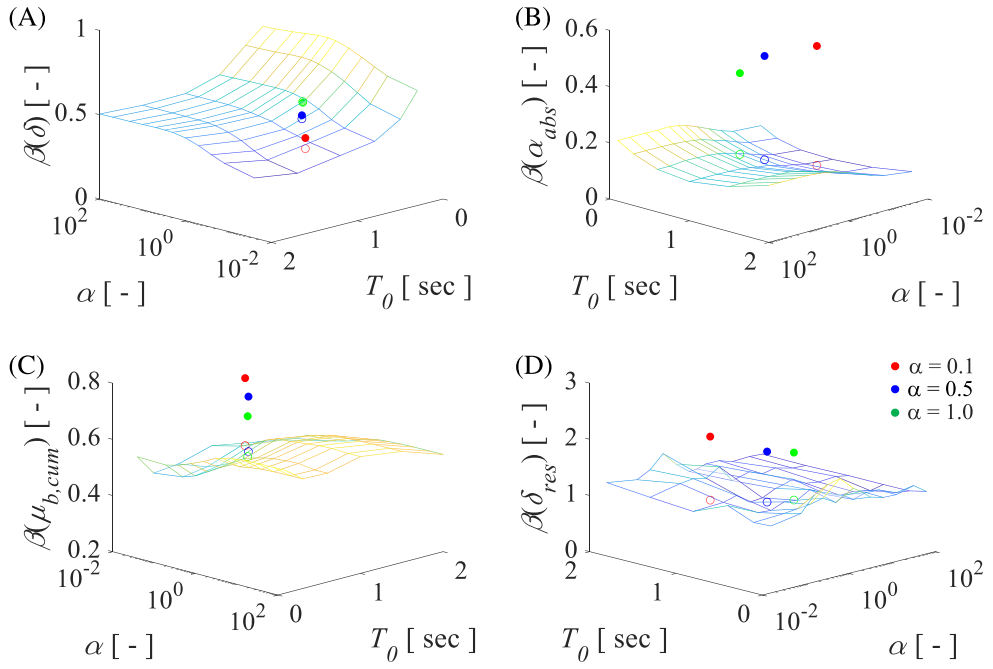

FIGURE 22 Seismic retrofitting of an RC MRF with BRBs. Comparison of the parametric analyses for SDOF and MDOF. Dispersion of the A, normalized peak displacement demand δ, B, normalized peak absolute accelerations demand α_{abs}, C, BRBF's normalized cumulative ductility demand $\mu_{b,cum}$, D, normalized residual displacement demand δ_{res} versus base shear ratio α, for different values of T_0 and of $\mu_{ft} = 4$ and $\mu_{bt} = 15$ [Colour figure can be viewed at wileyonlinelibrary.com]

TABLE 1 Newly designed dual steel MRF and BRBF

	Case 1			Case 2			Case 3		
	(T = 1.28 s, α = 0.1)			(T = 0.55 s, α = 1)			(T = 0.33 s, α = 3)		
Parameter	**MDOF**	**SDOF**	**Δ**	**MDOF**	**SDOF**	**Δ**	**MDOF**	**SDOF**	**Δ**
$GM(\delta)$	1.261	0.966	31%	1.665	1.362	22%	2.084	1.832	14%
$\beta(\delta)$	0.304	0.264	15%	0.485	0.504	4%	0.628	0.616	2%
$GM(\alpha_{abs})$	1.982	0.562	253%	0.877	0.318	176%	0.671	0.346	94%
$\beta(\alpha_{abs})$	0.458	0.162	183%	0.547	0.183	199%	0.249	0.178	40%
$GM(\mu_{b,cum})$	181.29	158.2	15%	108.63	102.1	6%	89.99	93.36	4%
$\beta(\mu_{b,cum})$	0.676	0.538	26%	0.639	0.566	13%	0.578	0.576	0%
$GM(\delta_{res})$	0.119	0.057	109%	0.176	0.09	96%	0.237	0.111	114%
$\beta(\delta_{res})$	2.853	2.361	21%	2.176	1.268	72%	2.02	1.01	100%

TABLE 2 Seismic retrofitting of an RC MRF with BRBs

	Case 1			Case 2			Case 3		
	(T = 1.10 s, α = 0.1)			(T = 0.79 s, α = 0.5)			(T = 0.64 s, α = 1)		
Parameter	**MDOF**	**SDOF**	**Δ**	**MDOF**	**SDOF**	**Δ**	**MDOF**	**SDOF**	**Δ**
$GM(\delta)$	1.561	1.064	47%	1.77	1.289	37%	1.957	1.439	36%
$\beta(\delta)$	0.439	0.377	16%	0.49	0.469	4%	0.523	0.531	2%
$GM(\alpha_{abs})$	1.487	0.299	397%	1.104	0.264	318%	0.924	0.255	262%
$\beta(\alpha_{abs})$	0.514	0.089	478%	0.482	0.112	330%	0.42	0.131	221%
$GM(\mu_{b,cum})$	186.63	199.69	7%	150.57	165.66	9%	135.78	152.68	11%
$\beta(\mu_{b,cum})$	0.771	0.531	45%	0.756	0.56	35%	0.71	0.566	25%
$GM(\delta_{res})$	0.246	0.23	7%	0.284	0.265	7%	0.302	0.253	19%
$\beta(\delta_{res})$	2.2	1.07	106%	1.919	1.02	88%	1.905	1.059	80%

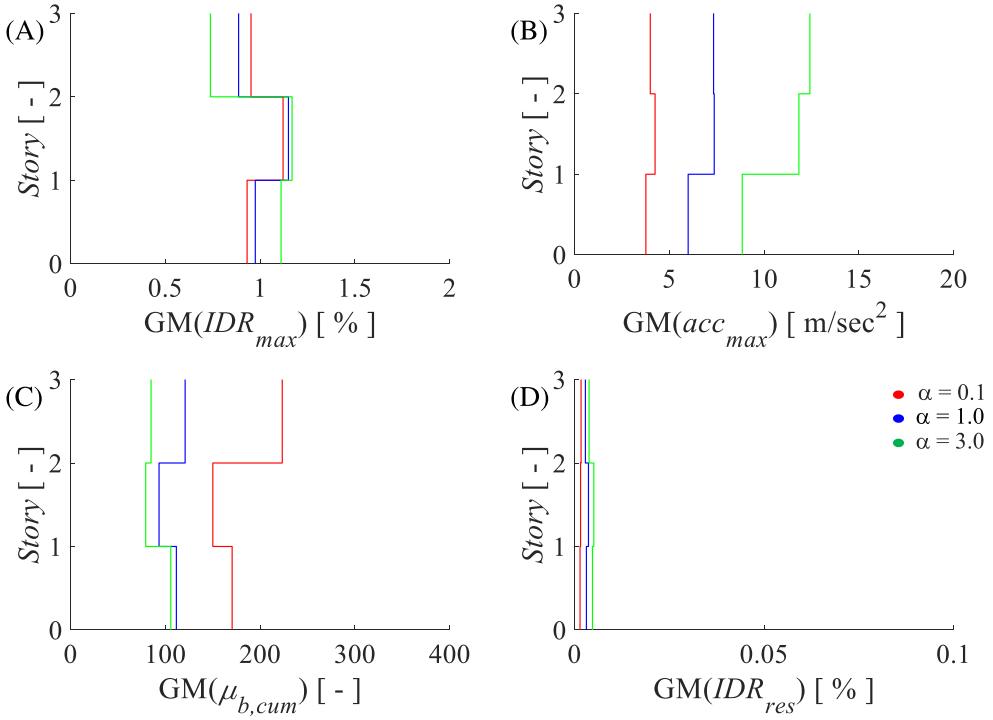

FIGURE 23 Newly designed dual steel MRF and BRBF. Story distribution of the geometric mean (GM) of the demand parameters for A, max inter-story drift ratio IDR_{max}, B, max story accelerations acc_{max}, C, cumulative ductility demand $\mu_{b,cum}$, D, residual inter-story drift ratio IDR_{res} for different values of the base shear ratio α and of $\mu_{ft} = 1$ and $\mu_{bt} = 10$ [Colour figure can be viewed at wileyonlinelibrary.com]

frame ($\mu_{ft} = 4$) and of the BRBs ($\mu_{bt} = 15$) produces (i) an increase of the difference between in terms of the GM of the normalized peak absolute accelerations demand α_{abs} and (ii) a reduction of the difference of the GM of the normalized residual displacement demand δ_{res}. Further studies are required to provide a careful quantification of the effects of these approximations in the estimation of the design parameters. Nevertheless, it can be concluded that the results of the parametric analysis of the SDOF systems are quite general and useful to draw important design recommendations.

In order to provide more insight into the response of the MDOF models, the results presented in this paragraph are complemented with those in Figures 23 and 24 showing the story distribution of the GM of the demand parameters (i.e., max inter-story drift ratio, max story accelerations, cumulative ductility demand, and residual inter-story drift

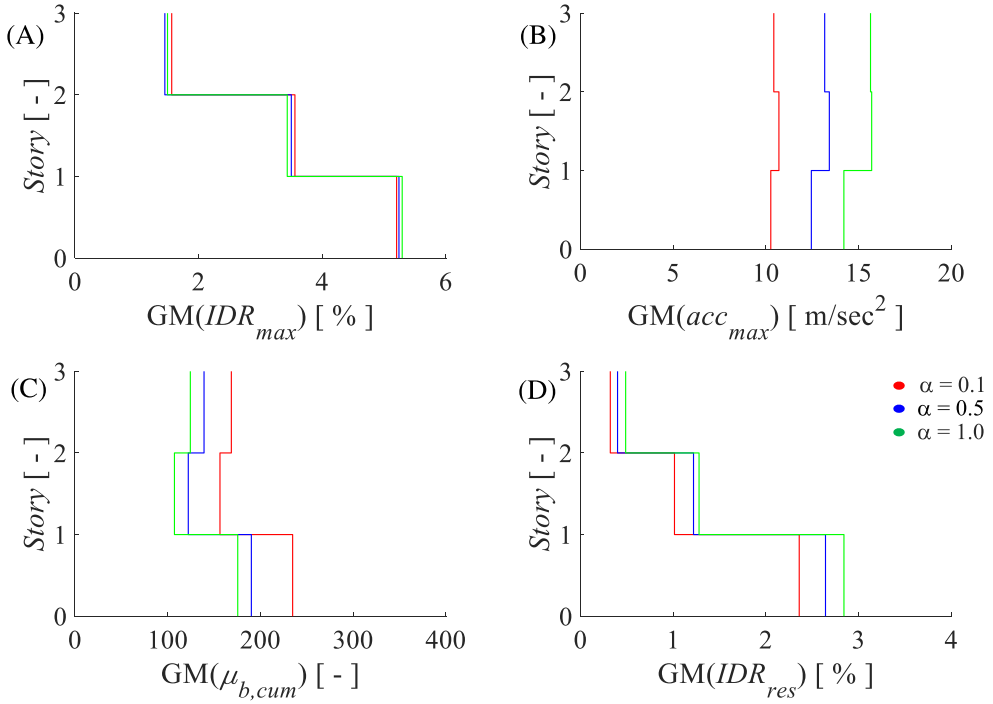

FIGURE 24 Seismic retrofitting of an RC MRF with BRBs. Story distribution of the geometric mean (GM) of the demand parameters for A, max inter-story drift ratio IDR_{max}, B, max story accelerations acc_{max}, C, cumulative ductility demand $\mu_{b,cum}$, D, residual inter-story drift ratio IDR_{res} for different values of the base shear ratio α and of $\mu_{ft} = 4$ and $\mu_{bt} = 15$ [Colour figure can be viewed at wileyonlinelibrary.com]

ratio) in correspondence of the design condition respectively for the newly designed dual steel MRF-BRBF case and for the RC MRF with BRBs, for the different values considered for the base shear ratio α. Among others, it is worth observing that in the case of the existing RC frame, there is a nonuniform distribution of the drift demands at the different stories. This is consequence of the design method used for the BRBs and of the behavior of the original, nonseismically design, RC frame. Conversely, in the case of the newly designed steel frame, a uniform drift distribution is obtained, thanks to the design approach followed.

6 | CONCLUSIONS

This paper presents an extensive parametric study investigating the seismic performance and residual capacity of dual systems consisting of buckling-restrained braced frames (BRBFs) coupled with moment-resisting frames (MRFs). An SDOF system assumption and a nondimensional problem formulation allow the estimation of the response of a wide range of configurations while limiting the number of simulations. This permits the evaluation of how the system properties, including different levels of the relative strength and ductility demand of the BRBF and MRF, affect the median demand and the dispersion of the normalized displacements, accelerations, residual displacements, and cumulative BRB ductility demand. Two realistic dual systems, consisting of MRFs and BRBFs modeled as MDOF systems, are also considered to evaluate the generality of the findings.

Based on the results of the study, the following conclusions are drawn. (1) Adding a very ductile BRBF in parallel to the MRF may result in residual displacements that may exceed the reparability limit of 0.5%, particularly for high values of α (i.e., the ratio between the base shear yielding forces of the BRBF and the MRF). The limit $\alpha_d = 3$ posed by SEI/ASCE 7–10 on the maximum values of α in dual systems gives values of the median residual-to-peak displacements ratio in the range 0.15–0.20, which may be excessive in some situations. In fact, for a maximum inter-story drift ratio of 4%, the expected residual drift would be of the order of 0.60%–0.80%, higher than the limit of reparability. (2) The dispersion of the residual displacements is very high, and this should be taken into account when assessing the probability of repairing a structure after an earthquake. (3) The median cumulative ductility demand of the BRBFs has an opposite trend of variation with α compared to the residual displacement, i.e., it decreases by increasing α. This result has also an impact on the choice of α in the design, because excessive accumulation of plastic deformations hampers the residual capacity of BRBs. (4) The observed results confirm the choice of a minimum value of $\alpha = 3$ for considering the system as dual. In fact, it is only for values of α less than 3 that many response parameters of interest (e.g., the peak displacements, the peak accelerations, and the cumulative ductility demand in the BRBs) exhibit a significant change of trend. (5) The SDOF model provides overall good estimates of the statistics of the response of the MDOF systems, with the limitations highlighted in the text. Amongst others, the main exception refers to the absolute accelerations, which are notably affected by higher order modes. Better agreement is observed for the case of the steel MRF, which is designed to remain elastic, whereas worse results are obtained for the case of the RC frame, due to the high nonlinear behavior of the systems that is not adequately described by the SDOF model.

Based on the conclusions and remarks on the results listed above, the following practical recommendations can be given to inform the design of MRF-BRBF dual systems. (1) Accelerations can be controlled by designing for α values higher than 1. The acceleration reduction is more significant in the case of the elastic frame, because in the case of the nonlinear frame, the yielding behavior already allows limiting accelerations. This has important implications for the performance of acceleration-sensitive components. (2) Similarly, the cumulative ductility demand on the BRB can be limited by increasing the values of α, i.e., by increasing the BRB frame contribution to the global response of the dual system. This has important implications for the residual capacity of the BRB devices when subjected to multiple earthquakes. (3) Increasing the BRB target ductility level has a different effect on accelerations and ductility demands. Although the former decrease for increased ductility levels, the latter increase. (4) The increase of the α value, which has beneficial effects in terms of control of acceleration and cumulative ductility demands, has, however, a detrimental effect on the residual displacements. Thus, the choice of the level of α depends on the performance objective.

ACKNOWLEDGEMENT

This research was partially supported by UK-India Education and Research Initiative (UKIERI) joint research program (Grant No. 2017-UGC-10070). Any opinions, findings, and conclusions or recommendations expressed in this paper are those of the authors and do not necessarily reflect the views of the funding agencies.

ORCID

Fabio Freddi https://orcid.org/0000-0003-2048-1166
Enrico Tubaldi https://orcid.org/0000-0001-8565-8917
Alessandro Zona https://orcid.org/0000-0002-3100-1802
Andrea Dall'Asta https://orcid.org/0000-0001-7482-9434

REFERENCES

1. Soong TT, Spencer BF. Supplemental energy dissipation: state-of-the-art and state-of-the-practice. *Eng Struct*. 2002;24(3):243-259.
2. Xie Q. State of the art of buckling-restrained braces in Asia. *J Constr Steel Res*. 2005;61(6):727-748.
3. Zona A, Dall'Asta A. Elasto-plastic model for steel buckling-restrained braces. *J Constr Steel Res*. 2012;68(1):118-125.
4. Gu Q, Zona A, Peng Y, Dall'Asta A. Effect of buckling-restrained brace model parameters on seismic structural response. *J Constr Steel Res*. 2014;98:100-113.
5. Tremblay R, Poncet L, Bolduc P, Neville R, DeVall R. Testing and design of buckling restrained braces for Canadian applications. *13th World Conference on Earthquake Engineering*, Vancouver, Canada; 1–6 August 2004.
6. Black CJ, Makris N, Aiken ID. Component testing, seismic evaluation and characterization of BRBs. *J Struct Eng*. 2002;130(6):880-894.
7. Ragni L, Zona A, Dall'Asta A. Analytical expressions for preliminary design of dissipative bracing systems in steel frames. *J Constr Steel Res*. 2011;67(1):102-113.
8. Freddi F, Tubaldi E, Ragni L, Dall'Asta A. Probabilistic performance assessment of low-ductility reinforced concrete frame retrofitted with dissipative braces. *Earthq Eng Struct Dyn*. 2013;42(7):993-1011.
9. Zona A, Ragni L, Dall'Asta A. Sensitivity-based study of the influence of brace over-strength distributions on the seismic response of steel frames with BRBs. *Eng Struct*. 2012;37(1):179-192.
10. Takeuchi T, Ida M, Yamada S, Suzuki K. Estimation of cumulative deformation capacity of buckling restrained braces. *J Struct Eng*. 2008;134(5):822-831.
11. Andrews BM, Fahnestock LA, Song J. Ductility capacity models for buckling-restrained braces. *J Constr Steel Res*. 2009;65(8-9):1712-1720.
12. Erochko J, Christopoulos C, Tremblay R, Choi H. Residual drift response of SMRFs and BRB frames in steel buildings designed according to ASCE 7-05. *J Struct Eng*. 2010;137(5):589-599.
13. Sabelli R, Mahin SA, Chang C. Seismic demands on steel braced-frame buildings with buckling-restrained braces. *Eng Struct*. 2003;25(5):655-666.
14. McCormick J, Aburano H, Ikenaga M, Nakashima M. Permissible residual deformation levels for building structures considering both safety and human elements. *14th World Conference on Earthquake Engineering*, Beijing, China; 12–17 October 2008.
15. CEN. EN 1998–1: 2005. Eurocode 8: design of structures for earthquake resistance—part 1: general rules, seismic actions and rules for buildings, *European Committee for Standardization*, Brussels, 2005.
16. Wigle VR, Fahnestock LA. Buckling-restrained braced frame connection performance. *J Constr Steel Res*. 2010;66(1):65-74.
17. Kiggins S, Uang CM. Reducing residual drift of buckling-restrained braced frames as dual system. *Eng Struct*. 2006;28(11):1525-1532.
18. Ariyaratana C, Fahnestock LA. Evaluation of buckling-restrained braced frame seismic performance considering reserve strength. *Eng Struct*. 2011;33(1):77-89.
19. Aukeman LJ, Laursen P. Evaluation of the ASCE 7-05 standard for dual systems: response history analysis of a tall buckling-restrained braced frame dual system. Structures Congress 2011: 2707–2717.
20. Xie Q. Dual system design of steel frames incorporating buckling-restrained braces. *14th World Conference on Earthquake Engineering*, Beijing, China; 12–17 October 2008.
21. Mehdipanah A, Mirghaderi SR, Tabatabaei SAR. Seismic performance of stiffness-based designed buckling-restrained braced frame and special moment-resisting frame dual systems. *Struct Infrastruct Eng*. 2016;12(8):918-935.
22. Pettinga D, Christopoulos C, Pampanin S, Priestley N. Effectiveness of simple approaches in mitigating residual deformations in buildings. *Earthq Eng Struct Dyn*. 2007;36(12):1763-1783.
23. Maley TJ, Sullivan TJ, Della CG. Development of a displacement-based design method for steel dual systems with buckling-restrained braces and moment-resisting frames. *J Earthq Eng*. 2010;14(S1):106-140.
24. Barbagallo F, Bosco M, Marino EM, Rossi PP. Seismic design and performance of dual structures with BRBs and semi-rigid connections. *J Constr Steel Res*. 2019;158:306-316.
25. Baiguera M, Vasdravellis G, Karavasilis TL. Dual seismic-resistant steel frame with high post-yield stiffness energy-dissipative braces for residual drift reduction. *J Constr Steel Res*. 2016;122:198-212.
26. ASCE/SEI 7–10. *Minimum design loads for buildings and other structures*. Reston, VA: American Society of Civil Engineers; 2010.
27. Montuori R, Nastri E, Piluso V. Influence of the bracing scheme on seismic performances of MRF-EBF dual systems. *J Constr Steel Res*. 2017;132:179-190.
28. Nastri E, Montuori R, Piluso V. Seismic design of MRF-EBF dual systems with vertical links: EC8 vs plastic design. *J Earthq Eng*. 2015;19(3):480-504.

29. Di Sarno L, Manfredi G. Seismic retrofitting with buckling restrained braces: application to an existing non-ductile RC framed building. *Soil Dyn Earthq Eng*. 2010;30(11):1279-1297.
30. Kotoky N, Freddi F, Ghosh J, Raghunandan M. BRBs uncertainty propagation in seismic retrofit of RC structures. *13th International Conference on Applications of Statistics and Probability in Civil Engineering*, Seoul, South Korea; 26–30 May 2019.
31. Guerrero H, Ruiz-García J, Ji T. Residual displacement demands of conventional and dual oscillators subjected to earthquake ground motions characteristic of the soft soils of Mexico City. *Soil Dyn Earthq Eng*. 2017;98:206-221.
32. Landolfo R. Assessment of EC8 provisions for seismic design of steel structures. *European Convention for Constructional Steelwork* (ECCS), *Technical Committee 13, Seismic design*, n. 131, Brussels, 2013.
33. Kim J, Seo Y. Seismic design of low-rise steel frames with buckling-restrained braces. *Eng Struct*. 2004;26(5):543-551.
34. Choi H, Kim J. Energy-based seismic design of buckling-restrained braced frames using hysteretic energy spectrum. *Eng Struct*. 2006; 28(2):304-311.
35. Freddi F, Padgett JE, Dall'Asta A. Probabilistic seismic demand modeling of local level response parameters of an RC frame. *Bull Earthq Eng*. 2017;15(1):1-23.
36. Ruiz-García J, Miranda E. Residual displacement ratios for assessment of existing structures. *Earthq Eng Struct Dyn*. 2006;35(3):315-336.
37. Porter KA. An overview of PEER's performance-based earthquake engineering methodology. *9th International Conference on Applications of Statistics and Probability in Civil Engineering*, San Francisco, USA; 6–9 July 2003.
38. Barenblatt GI. *Dimensional Analysis*. New York: Gordon and Breach Science Publishers; 1987.
39. Tubaldi E, Ragni L, Dall'Asta A. Probabilistic seismic response assessment of linear systems equipped with nonlinear viscous dampers. *Earthq Eng Struct Dyn*. 2015;44(1):101-120.
40. Makris N, Black CJ. Dimensional analysis of rigid-plastic and elasto-plastic structures under pulse-type excitations. *J Eng Mech*. 2004; 130(9):1006-1018.
41. Dimitrakopoulos E, Kappos AJ, Makris N. Dimensional analysis of yielding and pounding structures for records without distinct pulses. *Soil Dyn Earthq Eng*. 2009;29(7):1170-1180.
42. Karavasilis TL, Seo CY, Makris N. Dimensional response analysis of bilinear systems subjected to nonpulse-like earthquake ground motions. *J Struct Eng*. 2011;137(5):600-606.
43. Málaga-Chuquitaype C. Estimation of peak displacements in steel structures through dimensional analysis and the efficiency of alternative ground-motion time and length scales. *Eng Struct*. 2015;101:264-278.
44. Miranda E. Inelastic displacement ratios for displacement-based earthquake resistant design. 12th World Conference on Earthquake Engineering, Auckland, New Zealand; 30 January - 4 February 2000.
45. Whittaker A, Constantinou M. Seismic energy dissipation systems for buildings. In: Bertero VV, Bozorgnia Y, eds. *Earthquake Engineering, From Engineering Seismology to Performance-Based Engineering*. Boca Raton, Florida, USA: CRC Press; 2004.
46. Dall'Asta A, Ragni L, Tubaldi E, Freddi F. Design methods for existing RC frames equipped with elasto-plastic or viscoelastic dissipative braces. *13th Convegno Nazionale ANIDIS*; Bologna, Italy; 28 June – 2 July 2009.
47. Scozzese F, Tubaldi E, Dall'Asta A. Assessment of the effectiveness of multiple-stripe analysis by using a stochastic earthquake input model. *Bull Earthq Eng*. 2020;18(7):3167-3203.
48. Baker JW, Jayaram N, Shahi S. New ground motion selection procedures and selected motions for the PEER transportation research program. *PEER Technical Report*, Berkeley, CA; 2011/03.
49. McKenna F, Fenves GL, Scott MH. *OpenSees: Open System for Earthquake Engineering Simulation*. Berkeley, CA: Pacific Earthquake Engineering Center, University of California; 2006.
50. Chopra AK. *Dynamics of Structures: Theory and Applications to Earthquake Engineering*. Englewood Cliffs, NJ: Prentice-Hall; 1995 ISBN 0–13–855214–2.
51. Liossatou E, Fardis MN. Residual displacements of RC structures as SDOF systems. *Earthq Eng Struct Dyn*. 2015;44(5):713-734.
52. Smerzini C, Galasso C, Iervolino I, Paolucci R. Ground motion record selection based on broadband spectral compatibility. *Earthq Spectra*. 2014;30(4):1427-1448.
53. FEMA P695. *Quantification of Building Seismic Performance Factors. ATC-63 Project*. CA. USA: Applied Technology Council; 2008.
54. Ibarra LF, Medina RA, Krawinkler H. Hysteretic models that incorporate strength and stiffness deterioration. *Earthq Eng Struct Dyn*. 2005;34(12):1489-1511.
55. Lignos DG, Krawinkler H. Deterioration modelling of steel components in support of collapse prediction of steel moment frames under earthquake loading. *J Struct Eng*. 2011;137(11):1291-1302.
56. Zareian F, Medina RA. A practical method for proper modelling of structural damping in inelastic plane structural systems. *Comput Struct*. 2010;88(1):45-53.
57. Castro JM, Elghazouli AY, Izzuddin BA. Modelling of the panel zone in steel and composite moment frames. *Eng Struct*. 2005;27(1): 129-144.
58. Freddi F, Dimopoulos C, Karavasilis TL. Rocking damage-free steel column base with friction devices: design procedure and numerical evaluation. *Earthq Eng Struct Dyn*. 2017;46(14):2281-2300.

59. Morfuni F, Freddi F, Galasso C. Seismic performance of dual systems with BRBs under mainshock-aftershock sequences. *13th International Conference on Applications of Statistics and Probability in Civil Engineering*, Seoul, South Korea; 26–30 May 2019.
60. Bracci JM, Reinhorn AM, Mander JB. Seismic resistance of reinforced concrete frame structures designed for gravity loads: performance of structural system. *ACI Struct J*. 1995;92(5):597-608.

How to cite this article: Freddi F, Tubaldi E, Zona A, Dall'Asta A. Seismic performance of dual systems coupling moment-resisting and buckling-restrained braced frames. *Earthquake Engng Struct Dyn*. 2020;1–25. https://doi.org/10.1002/eqe.3332